
Learning Disentangled Representations in Signed Directed Graphs without Social Assumptions

Geonwoo Ko

Jeonbuk National University
geonwooko@jbnu.ac.kr

Jinhong Jung*

Jeonbuk National University
jinhongjung@jbnu.ac.kr

Abstract

Signed graphs are complex systems that represent trust relationships or preferences in various domains. Learning node representations in such graphs is crucial for many mining tasks. Although real-world signed relationships can be influenced by multiple latent factors, most existing methods often oversimplify the modeling of signed relationships by relying on social theories and treating them as simplistic factors. This limits their expressiveness and their ability to capture the diverse factors that shape these relationships. In this paper, we propose DINES, a novel method for learning disentangled node representations in signed directed graphs without social assumptions. We adopt a disentangled framework that separates each embedding into distinct factors, allowing for capturing multiple latent factors. We also explore lightweight graph convolutions that focus solely on sign and direction, without depending on social theories. Additionally, we propose a decoder that effectively classifies an edge’s sign by considering correlations between the factors. To further enhance disentanglement, we jointly train a self-supervised factor discriminator with our encoder and decoder. Throughout extensive experiments on real-world signed directed graphs, we show that DINES effectively learns disentangled node representations, and significantly outperforms its competitors in the sign prediction task.

1 Introduction

A signed graph represents a network consisting of a set of nodes and a set of positive and negative edges between nodes. Signed edges can model confrontational relations, such as trust/distrust, like/dislike, and agree/disagree; thus, signed graphs have been widely utilized to represent real-world relationships such as interpersonal interactions [1–3], user-item relations [4], and voting patterns [5–7]. Mining signed graphs have received considerable attention from data mining and machine learning communities [8] to develop diverse applications such as sign prediction [2, 6], link prediction [9, 10], node ranking [11–13], node classification [14], clustering [15], anomaly detection [16], community mining [17–19], etc.

Node representation learning in signed graphs encodes nodes into low-dimensional vector representations or embeddings while considering the signed edges between nodes. These node representations serve as features that can be utilized for various tasks, including those mentioned earlier. For this, many researchers have poured immense effort into developing intriguing methods, which are mainly categorized into *signed network embedding* and *signed graph neural network* (signed GNN). Signed network embedding methods [10, 20–24] take unsupervised approaches to the problem by optimizing their own likelihood functions that aim to place embeddings while preserving positive or negative relationships. On the other hand, signed GNNs [25–32] extract node representations using their own graph convolutions considering edge signs, and they are jointly trained with a downstream task in an end-to-end manner.

*Corresponding author

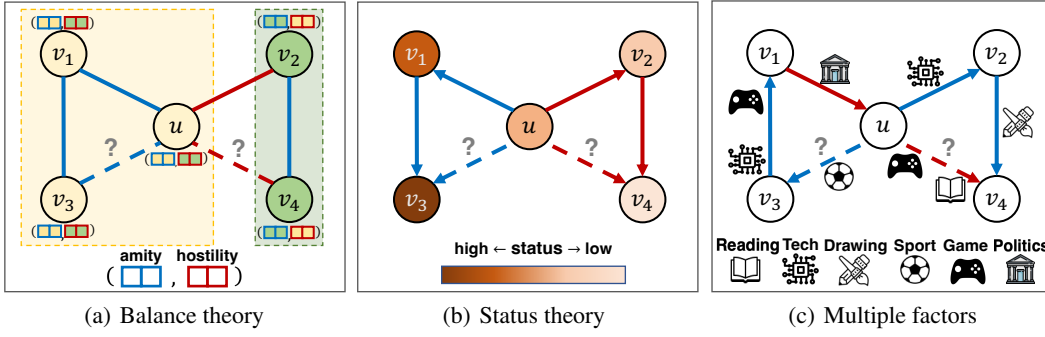


Figure 1: Illustration of how each social theory explains the sentiments of edges (u, v_3) and (u, v_4) where the blue edge represents a positive sentiment while the red edge represents a negative one. (a) According to the balance theory, (u, v_3) is positive because they belong to the same group where those nodes share similar semantics for both amity and hostility factors. Conversely, (u, v_4) is negative as they belong to different groups, resulting in opposite semantics for both factors. (b) The status theory explains the sentiments based on a status indicator where v_3 receives a positive sentiment due to its higher status compared to u while v_4 receives a negative sentiment due to its lower status than u . (c) However, these simplistic factors derived from the social theories are insufficient to fully comprehend the sentiments, which are influenced by intricate and diverse factors.

However, most existing methods heavily rely on social assumptions, such as those from structural balance theory² [33] or status theory³ [5], to model node embeddings considering signed edges, which limits the expressiveness of their representations as follows:

- A limitation of existing signed GNNs [25, 26, 30] is their narrow focus on amity (or friend) and hostility (or enemy) factors, neglecting other potentially influential factors. These methods only consider the information of potential friends or enemies for learning representations, adhering to the balance theory.
- Several methods [23, 25, 26, 31] disregard the directionality of edges by treating them as undirected although the raw datasets represent directed graphs, due to the assumption of undirected graphs in the balance theory. It should be noted that there is no guarantee that reciprocal edges have the same sign in real-world signed graphs [34].
- Network embedding methods [22, 24] use a set of random walk paths as input, where the signs are determined by the balance theory (i.e., + sign for even negative edges; − sign for odd). However, the interpretation of several signs can be misleading if the balance theory is unsuitable for explaining the corresponding paths⁴.
- Another approach is to optimize objective functions that are specifically tailored to capture triadic relationships satisfying either the balance theory [20, 25, 26, 29] or the status theory [20, 29]. However, this limited focus may restrict the ability of the models to capture other structural aspects of signed graphs, and secondarily, lead to inefficiency due to the computation of losses related to triadic patterns.

Thus, the dependence on the social assumptions oversimplifies the relationship between nodes by considering only a few simplistic factors such as amity/hostility or status, as shown in Figures 1(a) and 1(b). This hinders the ability of a learning model to capture the intricate and diverse nature of real-world signed relationships influenced by multiple latent factors. For example, Figure 1(c) depicts that the formation of edges in real-world signed graphs can be affected by the interaction (or correlation) between diverse factors. The node u positively thinks of v_3 as they may have the same interest on sport factor while it negatively considers v_4 because their opinions disagree on game and reading factors.

²The balance theory assumes that a network tends to be balanced, where individuals in the same group are more likely to share positive sentiments while those between the different groups are connected with negative sentiments, forming balanced triadic patterns such as my friend’s friend is a friend or my enemy’s friend is an enemy (see Figure 1(a)).

³The status theory postulates that individuals with higher status tend to form positive relationships, while those with lower status may experience more negative relationships (see Figure 1(b)).

⁴For example, the enemy of my enemy can be uncertain as weak balance theory [35] states triads with all enemies are balanced.

Table 1: Symbols.

Symbol	Definition
$\mathcal{G} = (\mathcal{V}, \mathcal{E})$	signed directed graph (or signed digraph) where \mathcal{V} and \mathcal{E} are sets of nodes and signed edges, resp.
$n = \mathcal{V} $	number of nodes
$m = \mathcal{E} $	number of edges
K	number of factors
L	number of layers
$d_{\text{in}}, d_{\text{out}}, d_l$	dimensions of input, output, and l -th embedding, respectively
\mathbf{x}_u	initial features of node u where $\mathbf{x}_u \in \mathbb{R}^{d_{\text{in}}}$
$\sigma(\cdot)$	non-linear activation function (e.g., \tanh)
\mathcal{D}	set of signed directions (or types of neighbor)
\mathcal{N}_u^δ	set of neighbors of node u for a given type $\delta \in \mathcal{D}$
\mathbf{z}_u	disentangled representation of node u , i.e., $\mathbf{z}_u = (\mathbf{z}_{u,1}, \dots, \mathbf{z}_{u,K})$ where $\mathbf{z}_{u,k} \in \mathbb{R}^{d_{\text{out}}/K}$ is k -th disentangled factor
\mathbf{H}_{uv}	$K \times K$ matrix representing the edge feature map of $u \rightarrow v$
p_{uv}	predicted probability of the sign of $u \rightarrow v$
$\lambda_{\text{disc}}, \lambda_{\text{reg}}$	strengths of discriminative and regularization losses, resp.
η	learning rate of an optimizer

Several methods [10, 21, 27, 32] have attempted to model node representations without relying on social theories, but their embeddings are encoded in a single embedding space, resulting in the entanglement of multiple latent factors and neglecting their potential diversity. Disentangled GNNs [36, 37] have emerged as a recent approach to explicitly model multiple factors in unsigned graphs, but their performance is limited when applied to signed graphs due to their lack of consideration for edge signs. In the case of signed graphs, MUSE [31] has focused on modeling multi-facet embeddings. However, its performance improvement comes from attention that considers high-order potential friends and enemies based on the balance theory, limiting scalability due to the significant increase in the number of multi-order neighbors as orders (or hops) increased.

How can we effectively learn multi-factored representations in a signed directed graph without any social assumptions? To address this question, we propose DINES (Disentangled Neural Networks for Signed Directed Graphs), a new GNN method for learning node representations in signed directed graphs without the social theories. To model multiple latent factors, we adopt a disentangled framework in our encoder design, which separates the embedding into distinct and disentangled factors. We then explore lightweight and simple graph convolutions that aggregate information from neighboring nodes only considering their directions and signs. On top of that, we propose a novel decoding strategy that constructs the edge feature by considering pairwise correlations among the disentangled factors of the nodes involved in the edge. We further enhance the disentanglement of factors by jointly optimizing a self-supervised factor discriminator with our encoder and decoder. Importantly, our approach explicitly models multiple latent factors without reliance on any social assumptions, thereby avoiding the aforementioned limitations, including the degradation of expressiveness and computational inefficiency associated with the use of the social theories.

We show the strengths of DINES through its complexity analysis and extensive experiments conducted on 5 real-world signed graphs with link sign prediction task, which are summarized as follows:

- **Accurate:** It achieves higher performance than the most accurate competitor, with **improvements of up to 3.1% and 6.5%** in terms of AUC and Macro-F1, respectively, in predicting link signs.
- **Scalable:** Its training and inference time **scales linearly** with the number of edges in real-world and synthetic signed graphs.
- **Speed-accuracy Trade-off:** It exhibits a **better trade-off** between training time and accuracy compared to existing signed GNN methods.

For **reproducibility**, the code and the datasets are publicly available at <https://github.com/geonwooko/DINES>. The rest of the paper is organized as follows. We provide related work and preliminaries in Sections 2 and 3, respectively. We present DINES in Section 4, followed by our experimental results in Section 5. Finally, we conclude in Section 6. The symbols used in this paper are summarized in Table 1.

2 Related Work

We review related work on representation learning for signed graphs, including approaches with and without social assumptions, as well as work on disentangled GNN for unsigned graphs. We further compare existing methods and DINES w.r.t. various properties in Appendix A.5.

Learning with social assumptions: Several learning models utilize the balance theory in constructing their inputs. SIDE [22] assigns a positive or negative sign to each node pair in truncated random walks, depending on whether the number of negative edges in the path is even or odd, respectively. Similarly, DDRE [24] employs random walk paths based on the balance theory as input for their expected matrix factorization with cross-noise sampling. For adversarial learning, ASiNE [23] generates fake edges based on the balance theory. SGCL [28] adopts contrastive learning based on graph augmentations using the balance theory.

In signed GNNs, most previous methods have relied on the balance theory to integrate edge signs into graph convolutions. SGCN [25], an extension of unsigned GCN [38], leverages the balance theory to model two representations, one for potential friends and another for potential enemies. SNEA [26] extends SGCN by adopting an attention mechanism to capture more important neighbors. SIDNET [30] addresses the over-smoothing issue of GCN [39] by using signed random walks [13] that adhere to the balance theory. MUSE [31] exploited a multi-facet attention mechanism on multi-order potential friends and enemies suggested by the balance theory.

Moreover, the social theories have been utilized in formulating structural loss functions. BESIDE [20] is a deep neural network that jointly optimizes the likelihood functions of being triangles and bridge edges (not forming triangles) based on the balance and status theories. SDGNN [29] is a signed GNN that also optimizes its objective functions of triangles based on the social theories. SGCN and SNEA additionally optimize a loss function based on extended structural balance theory [40].

As discussed in Section 1, these methods depend on the social theories for constructing inputs, designing graph convolutions, and formulating loss functions, which limits their expressiveness and ability to capture diverse latent factors inherent in signed relationships.

Learning without social assumptions: There have been a few methods proposed to learn node representations without the balance and status theories. SNE [21] adopts a log-bilinear model considering sign-typed embeddings, and optimizes the likelihood over truncated random walks. SLF [10] extends a latent factor model by considering sign and direction. Liu et al. [27] argued that the balance theory is too ideal to represent real-world social networks as it assumes a fully balanced graph is divided into only two groups. To address this, they introduced the k -group theory, allowing a graph to have up to k groups, and proposed GS-GNN that learns node embeddings based on the k -group theory. SigMaNet [32] introduces the Sign-Magnetic Laplacian to satisfy desirable properties of spectral GCNs for encoding both sign and direction (refer to [32] for details).

Although these methods learn node embeddings without using the balance and status theories, they may not effectively capture the diverse latent factors that influence real-world signed relationships. This is because they bundle information from a node’s neighborhood into a single holistic embedding, resulting in the entanglement of the latent factors and disregarding their potential diversity.

Disentangled graph neural networks: Several methods have been recently devised for modeling disentangled representations in unsigned graphs. DisenGCN [36] models multi-factored embeddings for each node, and performs neighborhood routing to disentangle node representations. DGCF [41] extends the disentangled approach to graph collaborative filtering so that it captures latent intents of relationships between users and items. DisGNN [42] employs such a strategy to model disentangled edge distributions. In addition to those methods, there are a few techniques proposed to encourage disentanglement based on independence [37] or self-supervision [42].

However, such GNNs are designed for only unsigned graphs, i.e., their graph convolutions do not consider edge signs, and thus their resulting representations have limited capacity for learning signed graphs.

3 Preliminaries

In this section, we introduce basic notations and a formal definition of the considered problem.

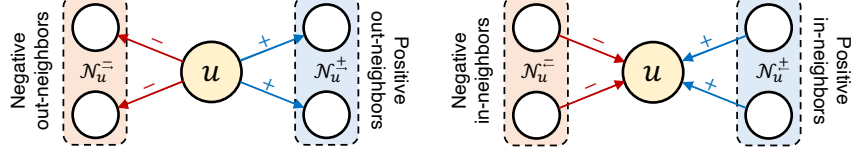


Figure 2: Concept of signed directed neighbors of node u .

3.1 Basic Notations

Signed directed graph: A signed directed graph $\mathcal{G} = (\mathcal{V}, \mathcal{E})$ consists of a set \mathcal{V} of nodes and a set \mathcal{E} of signed directed edges (i.e., each edge has a direction and a sign of positive or negative). We let $n = |\mathcal{V}|$ and $m = |\mathcal{E}|$ be the numbers of nodes and edges, respectively.

Signed directed neighbors: In a signed directed graph, the neighbors of a given node u are categorized by signs (+ and -) and directions ($\leftarrow_{(\text{in})}$ and $\rightarrow_{(\text{out})}$) [29]. Suppose $\mathcal{D} = \{\overset{+}{\rightarrow}, \overset{-}{\rightarrow}, \overset{+}{\leftarrow}, \overset{-}{\leftarrow}\}$ is the set of signed directions (e.g., $\overset{+}{\rightarrow}$ is the out-going direction with + sign). Then, \mathcal{N}_u^δ denotes the set of signed directed neighbors of node u with type $\delta \in \mathcal{D}$, and a node in \mathcal{N}_u^δ is called δ -neighbor of node u . The set of all neighbors of node u , regardless of directions and signs, is denoted by $\mathcal{N}_u = \bigcup_{\delta \in \mathcal{D}} \mathcal{N}_u^\delta$.

We illustrate the example of signed directed neighbors of node u in Figure 2. The sets of positive out-neighbors and in-neighbors are denoted by $\mathcal{N}_u^{\overset{+}{\rightarrow}}$ and $\mathcal{N}_u^{\overset{+}{\leftarrow}}$, respectively. The negative counterparts are expressed as $\mathcal{N}_u^{\overset{-}{\rightarrow}}$ and $\mathcal{N}_u^{\overset{-}{\leftarrow}}$, respectively.

3.2 Problem Definition

We describe the formal definition of the problem addressed in this paper as follows:

Problem 1. (Disentangled Node Representation in Signed Directed Graphs) Given a signed digraph \mathcal{G} and an initial feature vector $\mathbf{x}_u \in \mathbb{R}^{d_{\text{in}}}$ for each node u , the problem is to learn a disentangled node representation \mathbf{z}_u , expressed as a list of disentangled factors, i.e., $\mathbf{z}_u = (\mathbf{z}_{u,1}, \dots, \mathbf{z}_{u,K})$ such that $\mathbf{z}_{u,i} \neq \mathbf{z}_{u,j}$ for $i \neq j$ where $\mathbf{z}_{u,i}$ is the i -th factor of size $\frac{d_{\text{out}}}{K}$, d_* is the dimension of embeddings, and K is the number of factors.

4 Proposed Method

Figure 3 depicts the overall architecture of DINES which consists of three modules: 1) disentangled signed directed graph encoder (Section 4.1), 2) pairwise correlation decoder (Section 4.2), and 3) self-supervised factor-wise classification (Section 4.3).

Given a signed directed graph \mathcal{G} and an initial feature vector \mathbf{x}_u for each node u , our encoder learns the disentangled representation (or embedding) \mathbf{z}_u . Our encoder first disentangles \mathbf{x}_u into K latent factors, and then performs disentangled signed graph convolution (dsg-conv) layers for each factor space so that our model considers diverse latent factors for learning complicated relationships between nodes. The dsg-conv layer considers only directions and signs, i.e., it does not exploit any of the social theories for learning \mathbf{z}_u .

The disentangled embeddings are then fed forward to our decoder that predicts the sign of a given edge $u \rightarrow v$. To capture the influence of latent factors on the relationship between u and v , our decoder builds $\mathbf{H}_{uv} \in \mathbb{R}^{K \times K}$ called *edge feature map* which is based on the pairwise correlations between \mathbf{z}_u and \mathbf{z}_v . We further adopt a self-supervised approach to enhance the disentanglement of factors by classifying each factor of a node. Note that all of the modules are jointly trained in an end-to-end manner to effectively learn the node representations and downstream tasks.

4.1 Disentangled Signed Directed Graph Encoder

We describe our disentangled signed directed graph encoder. To explicitly model multiple latent factors, we adopt the disentangled learning framework in DisenGCN [36], originally designed

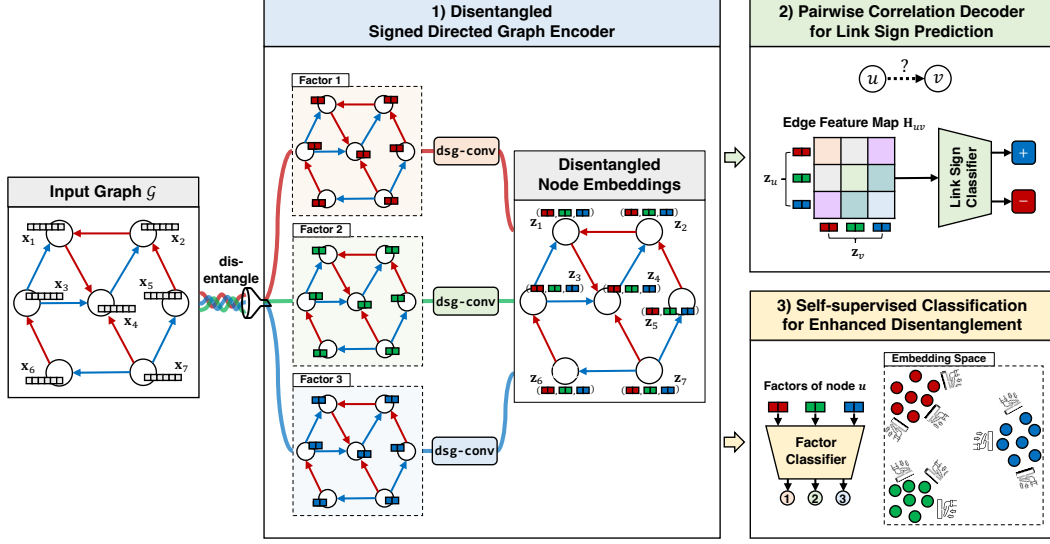


Figure 3: Overall structure of our proposed DINES which consists of 1) disentangled signed directed graph encoder, 2) pairwise correlation decoder, and 3) self-supervised classification where the number K of factors is 3.

for unsigned graphs. We extend this framework by incorporating simple and lightweight signed graph convolutions, allowing us to effectively encode distinct factors without relying on any social assumptions. Given a signed digraph \mathcal{G} and the initial feature $\mathbf{x}_u \in \mathbb{R}^{d_{in}}$ for each node u , our encoder aims to learn a disentangled representation $\mathbf{z}_u = (\mathbf{z}_{u,1}, \dots, \mathbf{z}_{u,K})$, as shown in Figure 3, where $\mathbf{z}_{u,i} \in \mathbb{R}^{\frac{d_{out}}{K}}$ is the i -th disentangled factor, and K is the number of factors. The overall procedure of the encoder is described in Algorithm 1.

Initial disentanglement (lines 1-5): To model various latent factors between nodes, we first separate the initial node features into K different factors. Specifically, for each node $v \in \mathcal{N}_u \cup \{u\}$, our encoder uses FC (fully-connected) layers to transform the feature vector \mathbf{x}_v into distinct subspaces as follows:

$$\mathbf{f}_{v,k}^{(0)} = \text{normalize}\left(\sigma(\text{FC}_k^{(0)}(\mathbf{x}_v))\right) = \frac{\tanh(\mathbf{W}_k^\top \mathbf{x}_v + \mathbf{b}_k)}{\|\tanh(\mathbf{W}_k^\top \mathbf{x}_v + \mathbf{b}_k)\|_2} \quad (1)$$

where $\mathbf{f}_{v,k}^{(l)}$ is the k -th latent factor of node v at step l , $\sigma(\cdot)$ is a non-linear activation function, $\mathbf{W}_k \in \mathbb{R}^{d_{in} \times \frac{d_0}{K}}$ is the weight parameters, and $\mathbf{b}_k \in \mathbb{R}^{\frac{d_0}{K}}$ is the bias parameters in the aspect of the k -th factor. Note that for all k , these parameters are differently set by random initialization before training, and the factors receive different supervision feedback from a decoder; thus, each subspace leads to distinct factors.

For $\sigma(\cdot)$ and $\text{normalize}(\cdot)$, any activation and normalization functions can be used, but we use the hyperbolic tangent $\tanh(\cdot)$ and the ℓ_2 -normalization due to the following reasons:

- The $\tanh(\cdot)$ allows each embedding to have values in a wider range compared to other functions such as ReLU and sigmoid, and it aids in increasing the difference in predicted scores between positive and negative edges. Thus, it has been commonly used in previous signed GNNs [25, 26, 28–30] to enhance the performance of link sign prediction.
- The ℓ_2 -normalization can prevent each embedding from exploding or collapsing, while also avoiding the risk that neighboring nodes with rich features overwhelm predictions, thereby ensuring numerical stability during training. Because of this, it has been widely used in existing disentangled GNNs [36, 37].

Disentangled signed graph convolution (lines 13-17): The initial factor $\mathbf{f}_{v,k}^{(0)}$ of node v is inadequate as the final disentangled factor $\mathbf{z}_{v,k}$ since it solely relies on the raw feature \mathbf{x}_v , and its information can be incomplete in the real world. Thus, we need to gather information from the

Algorithm 1 Encoder of DINES for node u

Input:

Set of signed directions: $\mathcal{D} = \{\vec{\rightarrow}, \vec{\leftarrow}, \vec{\uparrow}, \vec{\downarrow}\}$
 Feature vector of node u : $\mathbf{x}_u \in \mathbb{R}^{d_{in}}$
 Feature vectors of neighbors of u : $\{\mathbf{x}_v : v \in \mathcal{N}_u\}$ where $\mathcal{N}_u = \bigcup_{\delta \in \mathcal{D}} \mathcal{N}_u^\delta$
 Number of factors: K
 Number of layers: L

Output:

Disentangled representation of node u : $\mathbf{z}_u = (\mathbf{z}_{u,1}, \dots, \mathbf{z}_{u,K})$ where $\mathbf{z}_{u,k} \in \mathbb{R}^{\frac{d_L}{K}}$

```

1: for each  $v \in \mathcal{N}_u \cup \{u\}$  do
2:   for  $k = 1$  to  $K$  do                                     ▷ separate  $\mathbf{x}_v$  into  $K$  factors
3:      $\mathbf{f}_{v,k}^{(0)} \leftarrow \text{normalize}(\sigma(\text{FC}_k^{(0)}(\mathbf{x}_v)))$            ▷ Equation (1)
4:   end for
5: end for
6: for  $k = 1$  to  $K$  do                                           ▷ aggregate neighbors for each factor through  $L$  layers
7:   for  $l = 1$  to  $L$  do
8:      $\mathbf{f}_{u,k}^{(l)} \leftarrow \text{dsg-conv}_k^{(l)}(\{\mathbf{f}_{v,k}^{(l-1)} : v \in \mathcal{N}_u \cup \{u\}\})$ 
9:   end for
10: end for
11:  $\mathbf{z}_{u,k} \leftarrow \mathbf{f}_{u,k}^{(L)}$  for  $1 \leq k \leq K$                        ▷  $\mathbf{z}_{u,k}$  is a column vector of  $\frac{d_L}{K}$  size
12: return  $\mathbf{z}_u = (\mathbf{z}_{u,1}, \dots, \mathbf{z}_{u,K})$                              ▷ list of disentangled factors of node  $u$ 

13: function  $\text{dsg-conv}_k^{(l)}(\{\mathbf{f}_{v,k}^{(l-1)} : v \in \mathcal{N}_u \cup \{u\}\})$ 
14:    $\mathbf{m}_{u,k}^{(l)} \leftarrow \big\|_{\delta \in \mathcal{D}} \text{aggregate}_k(\{\mathbf{f}_{v,k}^{(l-1)} : v \in \mathcal{N}_u^\delta\})$ 
15:    $\mathbf{f}_{u,k}^{(l)} \leftarrow \text{update}_k(\mathbf{f}_{u,k}^{(l-1)}, \mathbf{m}_{u,k}^{(l)})$ 
16:   return  $\mathbf{f}_{u,k}^{(l)} \leftarrow \text{normalize}(\mathbf{f}_{u,k}^{(l)})$ 
17: end function

```

neighboring nodes of v so that the final factor comprehensively captures the underlying semantics of the node.

For this purpose, we design a disentangled signed graph convolution which is represented as a dsg-conv layer (lines 13-17):

$$\mathbf{f}_{u,k}^{(l)} = \text{dsg-conv}_k^{(l)}(\{\mathbf{f}_{v,k}^{(l-1)} : v \in \mathcal{N}_u \cup \{u\}\}) \quad (2)$$

where l indicates the l -th layer, and $\mathbf{f}_{v,k}^{(l-1)}$ is the k -th factor of neighbor v of node u from layer $l - 1$.

The convolution layer consists of 1) neighborhood aggregation, 2) update, and 3) normalization procedures, which are generally represented as follows:

$$\mathbf{m}_{u,k}^{(l)} = \big\|_{\delta \in \mathcal{D}} \text{aggregate}_k(\{\mathbf{f}_{v,k}^{(l-1)} : v \in \mathcal{N}_u^\delta\}) \quad (3)$$

$$\mathbf{f}_{u,k}^{(l)} = \text{update}_k(\mathbf{f}_{u,k}^{(l-1)}, \mathbf{m}_{u,k}^{(l)}) = \sigma(\text{FC}_k^{(l)}([\mathbf{f}_{u,k}^{(l-1)} \parallel \mathbf{m}_{u,k}^{(l)}])) \quad (4)$$

$$\mathbf{f}_{u,k}^{(l)} = \text{normalize}(\mathbf{f}_{u,k}^{(l)}) = \mathbf{f}_{u,k}^{(l)} / \|\mathbf{f}_{u,k}^{(l)}\|_2 \quad (5)$$

For each factor k , the aggregate_k function gathers the information of neighboring factors of node u with neighbor type $\delta \in \mathcal{D}$, and the disentangled message $\mathbf{m}_{u,k}^{(l)}$ is generated by concatenating all the aggregated results. The update_k function performs a non-linear transformation from the previous factor $\mathbf{f}_{u,k}^{(l-1)}$ and the message $\mathbf{m}_{u,k}^{(l)}$, leading to the updated factor $\mathbf{f}_{u,k}^{(l)}$. Specifically, their concatenation is fed into a fully-connected FC layer regarding factor k with a non-linear activation σ where the concatenation with $\mathbf{f}_{u,k}^{(l-1)}$ is considered as a simple form of skip connection [43] between the different layers. After then, it normalizes the resulting factor for numerical stability, as described above.

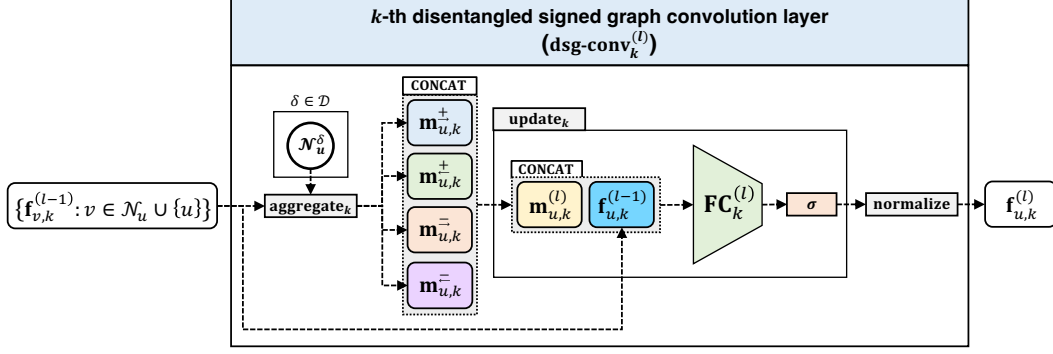


Figure 4: Concept of disentangled signed graph convolution (dsg-conv) at the l -th layer.

For $\text{aggregate}(\cdot)$ in Equation (3), as opposed to previous approaches [25, 26, 28–30], we aim to aggregate the neighborhood without depending on the assumptions from the structural balance or status theory. Thus, we adopt and investigate the following simple aggregators that gather the information of δ -neighbors where the type δ of neighbors is determined by only sign and direction (see Section 3.1).

- **Sum aggregator.** This simply adds the set of the k -th factor vectors of neighbors of node u without any normalization as follows:

$$\mathbf{m}_{u,k}^\delta := \sum_{v \in \mathcal{N}_u^\delta} \mathbf{f}_{v,k}$$

According to the previous study [44], the sum aggregator can provide a message that fully captures the local neighborhood structure as it is an injective function that distinctly maps a given multiset of features to a distinct output (or message).

- **Mean aggregator.** This calculates the element-wise mean of the set of the k -th factor vectors by dividing the number $|\mathcal{N}_u^\delta|$ of neighbors as follows:

$$\mathbf{m}_{u,k}^\delta := \sum_{v \in \mathcal{N}_u^\delta} \frac{1}{|\mathcal{N}_u^\delta|} \cdot \mathbf{f}_{v,k}$$

This approach is comparable to the convolutional rule employed in GCN [38], emphasizing the significance of normalization in constraining the magnitude of messages. The mean aggregator is characterized by its ability to capture the distribution of features within a given set by taking the average of individual element features [44].

- **Attention aggregator.** Unlike the mean aggregator which gives an equal weight to all neighbors, the attention aggregator assigns different weights to the neighbors and takes the weighted average as follows:

$$\mathbf{m}_{u,k}^\delta := \sum_{v \in \mathcal{N}_u^\delta} \alpha_k^\delta(u, v) \cdot \mathbf{f}_{v,k}$$

where v is a δ -neighbor of node u , and $\alpha_k^\delta(u, v)$ is their attention probability w.r.t. the k -th factor, i.e.,

$$\alpha_k^\delta(u, v) = \frac{\exp\left(\text{LeakyReLU}(\langle \mathbf{a}_k^\delta, [\mathbf{f}_{u,k} \parallel \mathbf{f}_{v,k}] \rangle)\right)}{\sum_{w \in \mathcal{N}_u^\delta} \exp\left(\text{LeakyReLU}(\langle \mathbf{a}_k^\delta, [\mathbf{f}_{u,k} \parallel \mathbf{f}_{w,k}] \rangle)\right)}$$

where $\langle \cdot, \cdot \rangle$ is an inner product of two vectors, and \mathbf{a}_k^δ is a trainable parameter vector of size $\frac{2d}{K}$.

- **Max pooling aggregator.** The max pooling aggregator takes element-wise maximum values of the set of factors as follows:

$$\mathbf{m}_{u,k}^\delta := \max(\{\mathbf{W}_k^\delta \cdot \mathbf{f}_{v,k} : v \in \mathcal{N}_u^\delta\})$$

Algorithm 2 Decoder of DINES for link sign prediction

Input:

Set of disentangled node representations: $\{\mathbf{z}_u : u \in \mathcal{V}\}$
Set of directed edges: \mathcal{E}

Output:

Set of predicted probabilities: $\{p_{uv} : (u \rightarrow v) \in \mathcal{E}\}$

1: **for each** $(u \rightarrow v) \in \mathcal{E}$ **do**

2: $\mathbf{Z}_u \leftarrow \text{CONCAT}(\mathbf{z}_u)$ and $\mathbf{Z}_v \leftarrow \text{CONCAT}(\mathbf{z}_v)$

3: $\mathbf{H}_{uv} \leftarrow \mathbf{Z}_u^\top \mathbf{Z}_v$

4: $p_{uv} \leftarrow \text{sigmoid}(\text{sum}(\mathbf{H}_{uv} \odot \mathbf{W}_s))$

5: **end for**

6: **return** $\{p_{uv} : (u \rightarrow v) \in \mathcal{E}\}$

▷ generate the edge feature map of $u \rightarrow v$
▷ predict the probability of a sign

where $\max(\cdot)$ is the element-wise max operator and $\mathbf{W}_k^\delta \in \mathbb{R}^{\frac{d}{K} \times \frac{d}{K}}$ is a trainable parameter matrix. The max aggregator aims to effectively capture representative elements of the neighboring set [43, 44] as it takes the important (or maximum) information for each element.

We stack L layers of the `dsg-conv` operation for each factor k (lines 6–10), and set $\mathbf{f}_{u,k}^{(L)}$ to $\mathbf{z}_{u,k}$ as the final disentangled factor where we set d_L to d_{out} (line 11). The disentangled representation of node u is expressed as a list of $\{\mathbf{z}_{u,k}\}$ (line 12), i.e., $\mathbf{z}_u = (\mathbf{z}_{u,1}, \dots, \mathbf{z}_{u,K})$. We apply our encoder to all nodes in order to obtain their final representations.

4.2 Pairwise Correlation Decoder for Sign Prediction

As the sentiment of an edge can be affected by correlations between factors (see Figure 1(c)), we propose a new decoding strategy that explicitly models pairwise correlations of disentangled factors and uses them as the edge’s feature for the link sign prediction task. The procedure of our decoder is described in Algorithm 2.

Pairwise correlation decoder (lines 1–5): Given the set $\{\mathbf{z}_u\}$ of disentangled representations and the set \mathcal{E} of directed edges, our decoder predicts the probability p_{uv} of the sign of each input edge $u \rightarrow v$. For a directed edge $u \rightarrow v$ to be predicted, our decoder first reshapes \mathbf{z}_u and \mathbf{z}_v as follows:

$$\mathbf{Z}_u = \text{CONCAT}(\mathbf{z}_u) = [\mathbf{z}_{u,1} \quad \dots \quad \mathbf{z}_{u,K}] \quad \mathbf{Z}_v = \text{CONCAT}(\mathbf{z}_v) = [\mathbf{z}_{v,1} \quad \dots \quad \mathbf{z}_{v,K}]$$

where $\mathbf{Z}_u \in \mathbb{R}^{\frac{d_{\text{out}}}{K} \times K}$ is a matrix horizontally concatenating the column vectors $\mathbf{z}_{u,k} \in \mathbb{R}^{\frac{d_{\text{out}}}{K} \times 1}$ from $k = 1$ to K . The dimension of \mathbf{Z}_v is the same as that of \mathbf{Z}_u . We then obtain pairwise correlations between factors as follows:

$$\mathbf{H}_{uv} = \mathbf{Z}_u^\top \mathbf{Z}_v = \begin{bmatrix} \langle \mathbf{z}_{u,1}, \mathbf{z}_{v,1} \rangle & \dots & \langle \mathbf{z}_{u,1}, \mathbf{z}_{v,K} \rangle \\ \vdots & \ddots & \vdots \\ \langle \mathbf{z}_{u,K}, \mathbf{z}_{v,1} \rangle & \dots & \langle \mathbf{z}_{u,K}, \mathbf{z}_{v,K} \rangle \end{bmatrix} \quad (6)$$

where $\mathbf{H}_{uv} \in \mathbb{R}^{K \times K}$ is a factor-to-factor correlation matrix, i.e., the inner product $\langle \mathbf{z}_{u,i}, \mathbf{z}_{v,j} \rangle$ is a scalar interpreted as a correlation between i -th factor of node u and j -th factor of node v for $1 \leq i, j \leq K$. We call \mathbf{H}_{uv} the edge feature map of edge $u \rightarrow v$.

After then, our decoder calculates a score (or logit) s_{uv} given \mathbf{H}_{uv} as the following:

$$s_{uv} = \text{sum}(\mathbf{H}_{uv} \odot \mathbf{W}_s) = \sum_{i=1}^K \sum_{j=1}^K w_{ij} \langle \mathbf{z}_{u,i}, \mathbf{z}_{v,j} \rangle \quad (7)$$

where $\text{sum}(\cdot)$ is a function summing all entries of an input matrix, $\mathbf{W}_s \in \mathbb{R}^{K \times K}$ is a learnable weight matrix, \odot is the element-wise multiplication (or the Hadamard product), and w_{ij} is (i, j) -th weight of \mathbf{W}_s . Note that our decoder learns $O(K^2)$ correlations with weights $\{w_{ij}\}$ as shown in Equation (7). Finally, the decoder computes the prediction probability as $p_{uv} = \text{sigmoid}(s_{uv})$ for the edge (line 4), and returns the set of predicted probabilities of all given edges (line 6).

Loss function for link sign prediction: The target task is considered a binary classification problem because it has two $+$ and $-$ classes. Thus, after computing the probability p_{uv} , DINES optimizes

the following standard binary cross entropy (bce) loss during training:

$$\mathcal{L}_{\text{bce}} = -\frac{1}{|\mathcal{E}|} \sum_{(u \rightarrow v) \in \mathcal{E}} (y_{uv} \log(p_{uv}) + (1 - y_{uv}) \log(1 - p_{uv})) \quad (8)$$

where \mathcal{E} is the set of training edges, and y_{uv} is the ground-truth of the sign of $u \rightarrow v$, i.e., $y_{uv} = 1$ for + sign, or $y_{uv} = 0$ for - sign. After the training phase of DINES is complete, the classifier predicts the sign of a test edge $u \rightarrow v$ as + sign if $p_{uv} \geq 0.5$; otherwise, it is classified as - sign.

Comparative Analysis: The conventional approach in an entangled framework for building the edge’s feature of two nodes u and v is to simply concatenate their corresponding embeddings [25–28, 30, 31]. Similarly, we could have followed the existing concatenation strategy, but such an approach is limited in fully exploiting the advantage of our disentangled representations. For example, suppose the edge feature is made by the naive concatenation of \mathbf{z}_u and \mathbf{z}_v , i.e., $\mathbf{h}_{uv} = \text{CONCAT}(\{\mathbf{z}_u, \mathbf{z}_v\}) \in \mathbb{R}^{2d_{\text{out}}}$. Then, the score s_{uv} is obtained with a trainable weight vector $\mathbf{w} \in \mathbb{R}^{2d_{\text{out}}}$ as follows:

$$s_{uv} = \langle \mathbf{w}, \mathbf{h}_{uv} \rangle = \sum_{k=1}^K \langle \mathbf{w}_{u,k}, \mathbf{z}_{u,k} \rangle + \sum_{k=1}^K \langle \mathbf{w}_{v,k}, \mathbf{z}_{v,k} \rangle \quad (9)$$

where $\mathbf{w}_{u,k} \in \mathbb{R}^{\frac{d_{\text{out}}}{K}}$ is the sub-vector of parameters corresponding to $\mathbf{z}_{u,k}$ in \mathbf{w} . Equation (9) implies that the concatenation strategy focuses on the information from each factor as $\langle \mathbf{w}_{u,k}, \mathbf{z}_{u,k} \rangle$, whereas our decoding strategy learns about correlations between factors as $w_{ij} \langle \mathbf{z}_{u,i}, \mathbf{z}_{v,j} \rangle$ according to Equation (7). Hence, our disentangled approach allows our model to leverage K^2 signals from the pairwise correlations of factors, which is more diverse than the naive concatenation strategy that utilizes only $2K$ signals from individual factors. We empirically demonstrate that our decoding strategy is more effective than the traditional one in Section 5.4 (see Table 6).

4.3 Self-supervised Factor-wise Classification

Although our encoder and decoder provide a framework that learns about disentangled factors and their correlations, this framework could be underperformed if we focus on only disentangling the embeddings, as in other disentangled GNNs [36]. Previous work [37, 42] claimed that such GNNs could fail to sufficiently diversify latent factors as the relationship between the factors is likely to be complicated. Thus, it is desirable to encourage the disentanglement between factors under the hypothesis that the representations of latent factors should be distinct.

In this work, we also follow the suggested direction for enhanced disentanglement. Specifically, we adopt a self-supervised approach utilized in [42], and investigate its effect on our purpose. The predefined (or pretext) task is to classify each factor of a node so that it aims to boost the difference across factors (i.e., well-disentangled factors should be distinguishable from each other). For each node u , we generate a pseudo label $y_{u,k}$ which is set to the factor index of $\mathbf{z}_{u,k}$, i.e., $y_{u,k} = k$ where $1 \leq k \leq K$. Then, we train a classifier for the factor-wise classification task by optimizing the following discriminative loss:

$$\mathcal{L}_{\text{disc}} = -\frac{1}{nK} \sum_{u \in \mathcal{V}} \sum_{k=1}^K \sum_{i=1}^K \mathbb{I}(y_{u,k} = i) \log \left(\text{softmax}_i(\text{FC}_{\text{disc}}(\mathbf{z}_{u,k})) \right) \quad (10)$$

where \mathcal{V} is the set of nodes, n is the number of nodes, K is the number of factors, $\text{softmax}_i(\cdot)$ is i -th probability after the softmax operation, and $\mathbb{I}(\cdot)$ is an indicator function that returns 1 if a given predicate is true, and 0 otherwise. $\text{FC}_{\text{disc}}(\cdot)$ consists of a weight matrix $\mathbf{W}_{\text{disc}} \in \mathbb{R}^{K \times \frac{d_{\text{out}}}{K}}$ and a bias vector $\mathbf{b}_{\text{disc}} \in \mathbb{R}^K$.

4.4 Final Loss Function

We jointly train the above discriminator on top of our encoder and decoder in an end-to-end scheme by optimizing the following loss function:

$$\mathcal{L} = \mathcal{L}_{\text{bce}} + \lambda_{\text{disc}} \mathcal{L}_{\text{disc}} + \lambda_{\text{reg}} \mathcal{L}_{\text{reg}} \quad (11)$$

where \mathcal{L}_{bce} is the cross entropy loss of Equation (8) of the decoder connected from the encoder, and $\mathcal{L}_{\text{disc}}$ is the discriminative loss of Equation (10) with its strength λ_{disc} . We further optimize the regularization loss \mathcal{L}_{reg} based on ℓ_2 -regularization (or weight decay) of model parameters to control overfitting where λ_{reg} is the strength of regularization.

Table 2: Data statistics of signed graphs. $|\mathcal{V}|$ and $|\mathcal{E}|$ indicate the number of nodes and edges, respectively. $|\mathcal{E}^s|$ is the number of edges having s sign where s is $+$ or $-$. $\rho(+)$ is the ratio of positive edges, i.e., $\rho(+)=|\mathcal{E}^+|/|\mathcal{E}|$.

Dataset	$ \mathcal{V} $	$ \mathcal{E} $	$ \mathcal{E}^+ $	$ \mathcal{E}^- $	$\rho(+)$
BC-Alpha	3,783	24,186	22,650	1,536	93.6
BC-OTC	5,881	35,592	32,029	3,563	90.0
Wiki-RFA	11,258	178,096	138,473	38,623	78.3
Slashdot	79,120	515,397	392,326	123,255	76.1
Epinions	131,828	841,372	717,667	123,705	85.3

4.5 Computational Complexity Analysis

We analyze the computational complexity of DINES in this section. In the following analysis, $n = |\mathcal{V}|$ and $m = |\mathcal{E}|$ are the numbers of nodes and edges, respectively. Below, K is the number of factors, L is the number of layers, and d_* is the size of dimensions where $*$ is a wildcard character.

Theorem 1 (Time Complexity). *The time complexity of DINES is $O(m + n)$ where L , K , and d are fixed constants, assuming all of d_* are set to d .*

Proof. *The time complexity of each step in DINES is summarized in Table 7 at Appendix A.1. The time complexities of our encoder and decoder are proved in Lemmas 1 and 2, respectively. It takes $O(m)$ to compute the cross entropy loss \mathcal{L}_{bce} . For computing \mathcal{L}_{disc} , $FC_{disc}(\cdot)$ takes $O(d + K)$ time, and $\text{softmax}(\cdot)$ takes $O(K)$ time. We only consider the case when the indicator function is true; thus, the total cost of \mathcal{L}_{disc} for all nodes and k is $O(dKn + K^2n) = O(dKn)$ where $K \leq d$. Therefore, the total time complexity is $O(m + n)$.*

Theorem 1 indicates that DINES is linearly scalable w.r.t. the number m of edges where $n \leq m$ in real-world graphs as shown in Table 2.

5 Experiments

In this section, we empirically analyze the effectiveness of our proposed DINES for the link sign prediction task on real-world signed graphs. We aim to answer the following questions:

- **Q1. Accuracy (Section 5.2).** How accurately does DINES predict the sign of a link compared to other state-of-the-art methods?
- **Q2. Effect of aggregators (Section 5.3).** How does each aggregator for the signed graph convolution affect the accuracy of DINES?
- **Q3. Ablation study (Section 5.4).** How does each module of DINES affect its performance in the link sign prediction task?
- **Q4. Effect of hyperparameters (Section 5.5).** How do DINES’s hyperparameters affect its performance in the link sign prediction task?
- **Q5. Qualitative study (Section 5.6).** Does the discriminative loss of DINES make factors more distinguishable in their embedding space?
- **Q6. Computational efficiency (Section 5.7).** Is our DINES linearly scalable w.r.t. the number of edges? Does our method provide a good trade-off between accuracy and training time?

5.1 Experimental Setting

We describe our experimental setting including datasets, competitors, training details, and hyperparameter settings.

Datasets: We conduct experiments on five signed social networks whose statistics are summarized in Table 2. BC-Alpha and BC-OTC [2] are who-trusts-whom networks of users on Bitcoin platforms. Wiki-RFA [7] is a signed network in Wikipedia where users vote for administrator candidates. Slashdot [3] is a signed social network on Slashdot, a technology news website where a user can

tag other users as friends or foes. Epinions [1] is an online social network on Epinions, a general consumer review site where a user can express trustworthiness on others based on their reviews. Note that all of the datasets are signed directed graphs. We provide more details of the datasets in Appendix A.2.

Competitors: We extensively compare our proposed method DINES to the following competitors.

- *Signed network embedding methods:* SNE [21], SIDE [22], BESIDE [20], SLF [10], ASiNE [23], and DDRE [24].
- *Disentangled unsigned GNN:* DisenGCN [36].
- *Signed GNNs:* SGCN [25], SNEA [26], SGCL [28], GS-GNN [27], SDGNN [29], SIDNET [30], MUSE [31] and SigMaNet [32].

We provide detailed information regarding the implementation of each competitor in Appendix A.4. We exclude unsigned network embedding methods such as Deepwalk [45], LINE [46], and Node2vec [47] since previous studies [20, 21, 29] have demonstrated that these methods are inferior to the methods using the sign information in the link sign prediction task.

Note that the original datasets are represented as signed directed graphs, and we aim to learn signed directed graphs without any modification to the datasets. Following [29, 30], we conduct experiments on all methods including ASiNE, SGCN, SNEA, and GS-GNN in signed directed graphs formed from the non-filtered raw data. For DisenGCN, we use only edges without signs for training because the model takes an unsigned graph as input.

Data split and evaluation metrics: We perform link sign prediction (i.e., predicting whether links are positive or negative), a standard benchmark task in signed graphs, to evaluate the performance of each model. For the experiments, we randomly split the edges by the 8:2 ratio into training and test sets. Note that the ratio of signed edges is skewed significantly towards positive edges as shown in Table 2. Considering the imbalance, we use AUC [48] and Macro-F1 [49] in percentage, as metrics of the task. For each metric, we repeat experiments 10 times with different random seeds and report average test results with standard deviations.

Implementation details: We utilize the Adam optimizer for training where η is its learning rate. We implement all models including our DINES in Python 3.9 using PyTorch 1.10. We use a workstation with Intel Xeon Silver 4215R and Geforce RTX 3090 (24GB VRAM).

Hyperparameter settings: For all tested models, we set the dimension of the final node embeddings to 64 so that the embeddings have an equal capacity for learning the downstream task. We also fix the number of epochs to 100 so that each model reads the same amount of data for training. For each method, we use 5-fold cross-validation to search for the best hyperparameters and compute the test accuracy with the validated ones. The search space of each hyperparameter of DINES is as follows: $\{4, 8, 16\}$ for the number K of factors, $\{2, 4, 6, 8\}$ for the number L of layers, $\{0.1, 0.5, 1\}$ for the strength λ_{disc} of the discriminative loss, and $\{0.01, 0.005, 0.001\}$ for the learning rate η and the strength λ_{reg} of regularization where validated results are reported in Appendix A.3. We follow the range of each hyperparameter reported in its corresponding paper for other models.

5.2 Performance of Link Sign Prediction

Predictive performance: We evaluate all methods on real-world signed graphs for the link sign prediction task where the results are summarized in Tables 3 and 4 in terms of AUC and Macro-F1, respectively. For DINES, the sum aggregator is used for its optimal performance (see its effect in Table 5). We observe the following from the tables:

- Our proposed DINES shows the best performance among all tested methods in terms of both metrics across all datasets. Compared to the second-best results, our approach improves AUC by up to 3.1% and Macro-F1 by up to 6.5%, respectively.
- The performance of DisenGCN, an unsigned GCN, is much worse than that of DINES in most datasets. This result implies that it is important to consider the information from signs even in the disentangled framework.
- DINES outperforms methods relying on the balance or status theories (e.g., SIDE, BESIDE, SGCN, SNEA, SDGNN, and MUSE). This result validates that node embeddings are effectively trained through our disentangled approach without any assumption from the theories.

Table 3: Our DINES exhibits the best performance of link sign prediction in terms of AUC. The best result is marked in boldface, and the second-best result is underlined. The % diff means how much the best accuracy improved over the second-best accuracy. The o.o.m. stands for out-of-memory error.

AUC	BC-Alpha	BC-OTC	Wiki-RFA	Slashdot	Epinions
SNE	79.4±1.5	82.8±1.8	70.8±1.5	69.8±1.4	82.4±2.0
SIDE	81.8±1.0	83.9±0.6	73.3±1.0	80.4±0.3	91.0±0.3
BESIDE	89.9±0.6	91.9±0.6	<u>90.3±0.2</u>	<u>90.0±0.1</u>	93.9±0.1
SLF	86.5±0.9	88.2±1.1	89.9±0.3	88.6±0.1	90.9±0.2
ASiNE	82.5±1.4	83.0±0.7	70.9±0.7	o.o.m.	o.o.m.
DDRE	88.4±0.8	91.3±0.5	89.1±0.2	89.0±0.1	<u>94.0±0.1</u>
DisenGCN	84.4±1.7	86.9±1.1	70.2±1.6	73.7±1.3	86.6±0.6
SGCN	86.0±0.8	88.2±0.7	77.0±0.3	86.8±0.1	90.7±0.2
SNEA	<u>90.1±0.7</u>	90.7±0.7	88.0±0.2	75.8±3.3	84.1±0.5
SGCL	89.2±0.9	91.6±0.7	90.1±0.2	87.7±0.9	93.5±0.3
GS-GNN	88.5±0.7	91.6±0.4	85.5±0.4	88.2±0.1	92.7±0.1
SDGNN	89.2±0.6	91.5±0.5	89.3±0.3	88.2±0.2	92.9±0.8
SIDNET	89.4±0.6	92.0±0.8	89.8±0.1	89.2±0.1	<u>94.0±0.2</u>
MUSE	89.7±0.9	<u>92.2±0.8</u>	90.1±0.3	o.o.m.	o.o.m.
SigMaNet	86.6±0.7	89.4±0.6	86.2±0.2	84.8±0.1	91.1±0.3
DINES (Ours)	92.8±0.8	95.1±0.7	91.3±0.3	92.7±0.2	96.7±0.1
% diff	3.0%	3.1%	1.1%	2.8%	2.9%

Table 4: Our DINES also shows the best performance in terms of Macro-F1.

Macro-F1	BC-Alpha	BC-OTC	Wiki-RFA	Slashdot	Epinions
SNE	65.2±1.7	72.2±1.9	61.6±1.3	62.2±1.0	73.6±2.9
SIDE	62.7±1.7	69.1±1.1	53.4±2.1	68.1±1.7	81.2±0.6
BESIDE	72.7±1.0	79.0±1.0	78.5±0.2	79.1±0.1	86.3±0.1
SLF	74.0±1.2	78.9±1.0	<u>79.0±0.2</u>	<u>79.2±0.1</u>	84.0±0.6
ASiNE	61.6±1.8	67.0±1.5	52.8±0.4	o.o.m.	o.o.m.
DDRE	74.9±1.6	79.1±0.6	77.3±0.3	77.8±0.0	86.3±0.1
DisenGCN	63.2±1.8	73.1±1.8	49.2±2.5	63.6±4.2	76.5±0.6
SGCN	66.7±1.7	73.5±1.9	65.1±1.0	76.0±0.3	75.9±0.2
SNEA	73.1±1.8	77.3±1.3	76.1±0.2	43.2±0.0	77.5±0.9
SGCL	72.2±3.9	76.0±1.3	67.4±1.0	67.3±2.5	80.0±1.9
GS-GNN	73.7±1.6	80.7±0.7	71.5±1.9	77.3±0.3	<u>86.9±0.1</u>
SDGNN	73.9±1.5	<u>80.8±0.7</u>	77.8±0.5	77.1±0.4	86.3±0.3
SIDNET	<u>75.2±1.5</u>	79.5±1.0	77.7±0.6	78.4±0.2	85.8±0.2
MUSE	73.9±1.5	80.6±0.7	78.6±0.2	o.o.m.	o.o.m.
SigMaNet	72.0±1.6	77.8±0.9	74.8±0.3	74.4±0.2	82.4±0.3
DINES (Ours)	80.1±1.7	85.3±1.0	79.6±0.7	82.7±0.6	89.7±0.5
% diff	6.5%	5.5%	0.8%	4.0%	3.2%

- Note that the performance of our DINES is significantly better than that of other models in terms of Macro-F1 (i.e., the mean of per-class F1 scores). This result implies DINES is able to more accurately distinguish the sign of a given edge even for heavily imbalanced data as shown in Table 2.

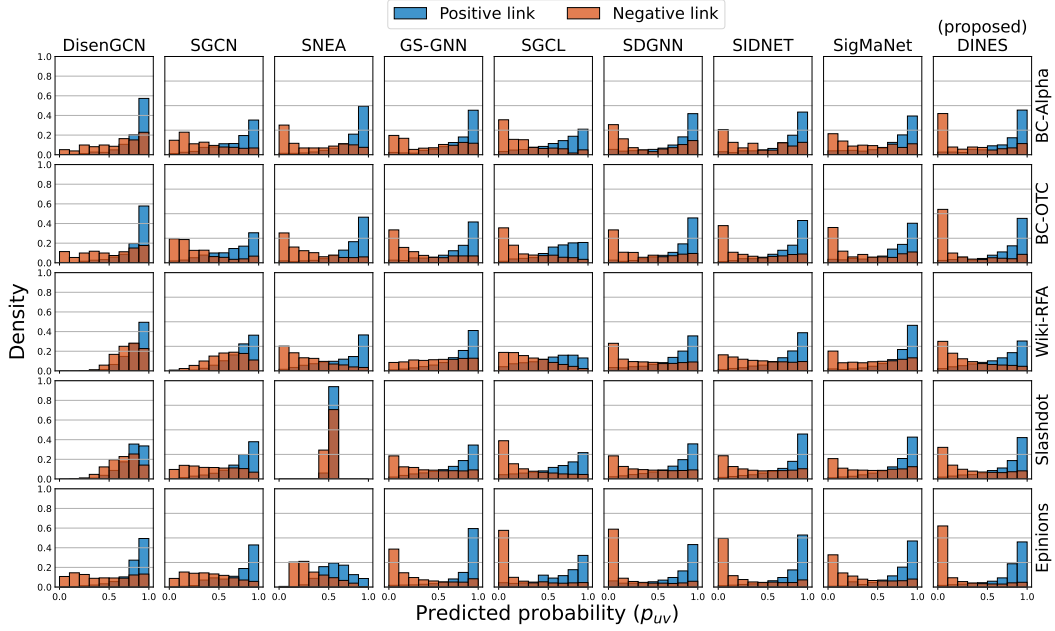


Figure 5: Distribution of predicted probabilities p_{uv} of each model. Our DINES predicts the probabilities more confidently and precisely than other methods as the distributions of DINES are more sharply U-shaped.

Table 5: Effect of different aggregators such as sum, max, mean, and attention on the performance of DINES. The sum aggregator consistently achieves the best accuracy across all datasets.

Metric	Variants	BC-Alpha	BC-OTC	Wiki-RFA	Slashdot	Epinions
AUC	DINES-SUM	92.8±0.8	95.1±0.7	91.3±0.3	92.7±0.2	96.7±0.1
	DINES-MAX	92.1±0.6	94.6±0.5	91.2±0.1	92.0±0.2	96.7±0.2
	DINES-MEAN	91.8±0.8	94.4±0.6	90.3±0.2	91.1±0.3	96.4±0.2
	DINES-ATTN	92.3±0.5	94.5±0.5	90.3±0.6	91.2±0.3	96.4±0.2
Macro-F1	DINES-SUM	80.1±1.7	85.3±1.0	79.6±0.7	82.7±0.6	89.7±0.5
	DINES-MAX	77.0±1.5	83.9±1.3	78.8±1.4	81.3±0.6	89.2±0.5
	DINES-MEAN	76.7±1.8	83.5±0.9	77.7±1.2	79.9±0.8	88.7±0.5
	DINES-ATTN	76.7±1.8	84.0±1.0	78.4±0.9	80.4±0.9	88.9±0.4

Distribution of predicted probabilities: We further analyze the distribution of predicted probabilities p_{uv} of each GNN model’s classifier for given test edges (u, v) , as shown in Figure 5, where MUSE is not considered due to its inability to handle large datasets. Note that a desirable classifier should compute high (or low) scores for positive (or negative) edges so that the distribution for the positive (or negative) class should be left (or right) skewed, i.e., a U-shaped distribution is desirable.

As demonstrated in Figure 5, the distributions of DINES are more distinct than those of other methods, especially at the leftmost and the rightmost ends. Specifically, our method predicts negative signs more confidently as well as positive signs compared to other state-of-the-art methods such as GS-GNN, SDGNN, and SIDNET. Note that DisenGCN produces an undesirable distribution for negative edges compared to other signed GNNs, implying that it is crucial to use the sign information for learning.

5.3 Effect of Aggregators

We examine the effect of aggregators such as sum, mean, max, and attention on DINES in the link sign prediction task. Table 5 demonstrates that the sum aggregator outperforms the others across all datasets. The primary distinction lies in the normalization of gathered message features. The mean,

Table 6: Result of the ablation study. Combined with disentanglement (D), pairwise correlations (P), and self-supervised classification (S), DINES provides the best accuracy for most datasets in terms of AUC and Macro-F1.

Metric	Variants	BC-Alpha	BC-OTC	Wiki-RFA	Slashdot	Epinions
AUC	DINES	92.8±0.8	95.1±0.7	91.3±0.3	92.7±0.2	96.7±0.1
	DINES-S	92.5±0.9	94.8±0.4	91.0±0.2	91.6±0.1	96.3±0.2
	DINES-SP	90.7±0.5	92.6±0.5	90.9±0.1	90.7±0.1	95.6±0.1
	DINES-SPD	89.8±0.6	92.3±0.5	90.5±0.1	90.1±0.1	95.1±0.2
Macro-F1	DINES	80.1±1.7	85.3±1.0	79.6±0.7	82.7±0.6	89.7±0.5
	DINES-S	79.2±0.7	85.4±0.7	79.0±1.1	81.5±1.1	88.7±0.6
	DINES-SP	75.5±1.5	81.9±0.6	79.0±0.3	79.7±0.2	88.0±0.1
	DINES-SPD	75.8±1.5	81.7±0.9	79.0±0.4	79.4±0.3	87.4±0.2

max, and attention aggregators apply their own normalization, whereas the sum aggregator does not. According to [44], this allows the sum aggregator to fully capture the structural information from the local neighborhood of a node, which may be compressed or condensed by the normalization in mean or max functions. In other words, the sum aggregator is injective, producing distinct messages from a multiset of neighboring features, unlike the others. Thus, the sum aggregator can offer more expressive features, particularly in capturing such a local structure.

Especially, the local neighborhood information of a node is highly related to the node’s degree. Based on our further investigation in Appendix A.6, we found that the magnitude of a gathered message using the sum aggregator exhibits a nearly perfect positive correlation with the degree, unlike other aggregators. This implies that the degree information is effectively distributed across the message feature of the sum aggregator such that the norm of the feature is proportional to the degree. As a result, the sum aggregator produces informative features that encode the degree information, enabling our model to effectively learn from the data and achieve superior performance. This result aligns with the in-depth analysis conducted in [50], which highlights node degrees as powerful features for the link sign prediction task.

5.4 Ablation Study

We conduct an ablation study to verify the effect of each module in DINES: disentanglement (D), pairwise correlation decoder (P), and self-supervised classification (S). For the study, we define the following variants of DINES:

- **DINES-S** excludes the self-supervised factor classification from DINES.
- **DINES-SP** excludes the pairwise decoding strategy from DINES-S. It simply concatenates the embeddings of two nodes for the edge feature, i.e., $\text{CONCAT}(\{\mathbf{z}_u, \mathbf{z}_v\})$ for a given edge $u \rightarrow v$.
- **DINES-SPD** excludes the disentanglement functionality from DINES-SP. It is equivalent to DINES-SP with $K = 1$.

Table 6 shows the result of the ablation study in terms of AUC and Macro-F1 of the link sign prediction task. Note that DINES achieves the best performance when all the modules are combined. We have the detailed observations as follows:

- DINES-S slightly underperforms compared to DINES for all datasets except the BC-OTC dataset, implying the enhanced disentanglement from the self-supervised factor classification is helpful for the performance.
- Regarding the effect of our decoding strategy, DINES-SP performs much worse than DINES-S, especially in the BC-Alpha and BC-OTC datasets. This result indicates that edge features based on our pairwise correlation are effective for the task, compared to the naive concatenation strategy.
- The disentanglement framework is also beneficial as DINES-SP performs better than DINES-SPD in most datasets.

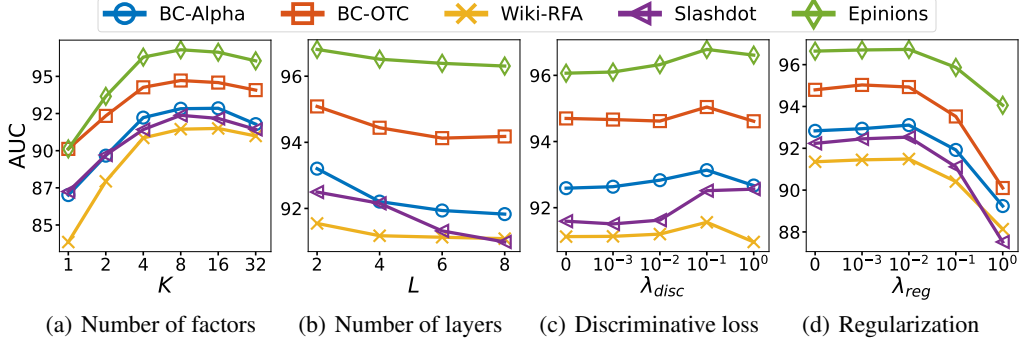


Figure 6: Effects of hyperparameters of DINES where (a) K is the number of factors, (b) L is the number of layers, (c) λ_{disc} is the strength of the discriminative loss, and (d) λ_{reg} is the strength of regularization.

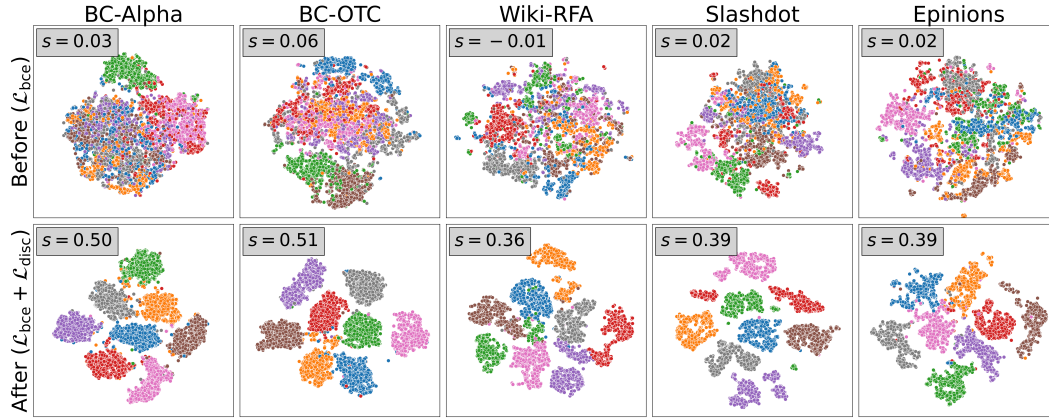


Figure 7: Visualization of disentangled node embeddings of DINES before or after the discriminative loss \mathcal{L}_{disc} is applied (best viewed in color).

5.5 Effect of Hyperparameters

We investigate the effects of hyperparameters K , L , λ_{disc} , and λ_{reg} of DINES as shown in Figure 6. For each hyperparameter, we vary its value while holding the other hyperparameters at the values obtained from the best settings.

- Figure 6(a) shows the effect of the number of factors, which is a crucial hyperparameter of DINES as it controls the factors between nodes. When $K = 1$ and 2 , the performance is poor, while it tends to improve as the value of K increases, implying that modeling latent and intricate relationships between nodes through the use of multiple factors is beneficial for enhancing performance. However, the performance is degraded when $K = 32$ because the dimension of each factor is too small. It's worth noting that this issue does not arise when the dimension is sufficient, as shown in Figure 11.
- Figure 6(b) demonstrates that DINES generally performs better when the number of L of layers is 2.
- In general, too small or large values of λ_{disc} are not a good choice because of their poor performances, as shown in Figure 6(c).
- Figure 6(d) indicates that if the value of λ_{reg} is greater than 0.01, then it adversely affects the performance of DINES as the model is heavily regularized.

5.6 Qualitative Analysis

We qualitatively analyze how the discriminative loss \mathcal{L}_{disc} of DINES affects its disentangled representation learning. For this purpose, we use t-SNE [51] to visualize disentangled node embeddings for each factor with a distinct color. Figure 7 demonstrates the visualization results for each dataset.

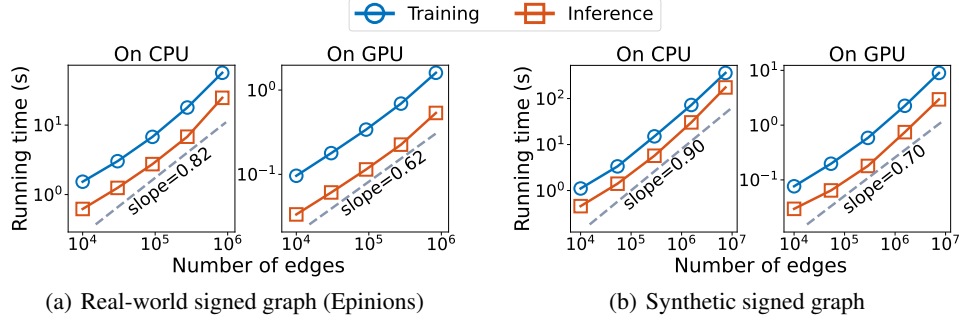


Figure 8: Scalability of DINES. The training and inference time of DINES shows linear scalability w.r.t. the number of edges in both real-world and synthetic signed graphs.

As expected by the motivation of $\mathcal{L}_{\text{disc}}$, DINES with the loss in the below sub-plots forms more distinct clusters for each factor on the projected space than that without the loss in the above sub-plots across all the datasets. The factors with the same class are agglomerated, and those between other classes are detached. We further numerically measure the cluster’s cohesion for each factor in terms of silhouette coefficient [52], and compute the average score s of silhouette coefficients of all clusters. As shown in the figure, the score s dramatically improves for all the datasets. Especially, the improvements of s in the BC-Alpha and BC-OTC datasets are significant, and the clusters of DINES with the loss are more distinguishable. All of the results verify the effectiveness of the discriminative loss $\mathcal{L}_{\text{disc}}$ that enhances the disentanglement of DINES’s node embeddings.

5.7 Computational Efficiency

In this section, we evaluate the computational efficiency of our proposed DINES in terms of scalability and trade-off.

Scalability: We investigate the scalability of DINES between its running time and the number m of edges on real-world and synthetic signed graphs. For the experiment, we select the Epinions dataset which is the largest real-world graph used in this work, and generate a synthetic signed graph whose number of edges is greater about $10\times$ than that of the Epinions by using a signed graph generator [53] to evaluate the scalability on a larger graph. We then extract principal submatrices by slicing the upper left part of the adjacency matrix so that m ranges from about 10^4 to the original number of edges in each of the real and synthetic graphs, respectively. We conduct the experiment on a CPU (i.e., sequential processing) and a GPU (i.e., parallel processing), respectively, to look into the performance in each environment. We report the inference or training time per epoch on average (i.e., the average time over 100 epochs). Note that the training time includes time for the optimization (backward) phase as well as the inference (forward) phase.

As shown in Figure 8, the inference time of DINES increases linearly with the number m of edges in both real-world and synthetic graphs, which empirically verifies the result of Theorem 1. Notice that the training time of DINES also shows a similar tendency to the inference time. Moreover, DINES using a GPU is much faster than that using a CPU due to the GPU’s parallel processing, showing lower slopes in both settings. These results indicate our DINES is scalable linearly w.r.t. the number of edges.

Accuracy v.s. Training Time: We further analyze the trade-off between accuracy and training time of all GNN methods including DINES. For each dataset, we train a model for 100 epochs (i.e., for training, all models are given an equal opportunity to read the dataset in the same number of epochs), and report the total training time on a GPU and the test accuracy in AUC, as shown in Figure 9. Note DINES achieves the best accuracy while showing fast training time compared to other methods (i.e., it is closest to the best point marker across most datasets). The reason is that our model leverages the correlation of multiple factors to enhance learning performance, and our approach employs lightweight graph convolutions without requiring the optimization of additional structural losses, in contrast to SGCN, SENA, and SDGNN.

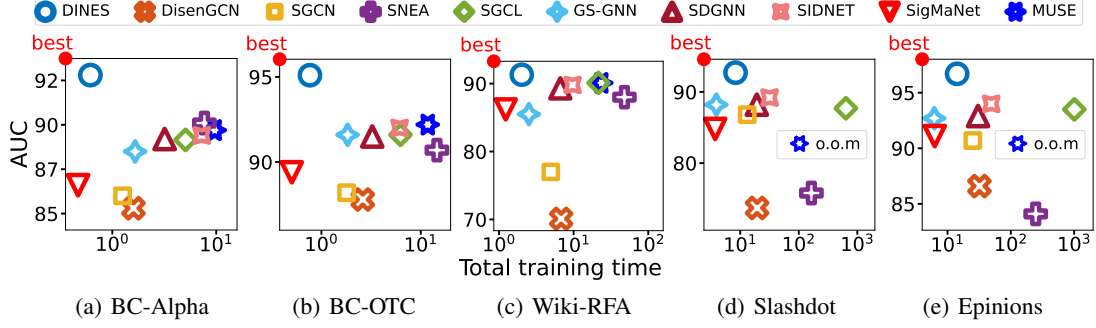


Figure 9: Trade-off between accuracy and running time where the upper left marker indicates the best trade-off. Our method DINES provides the best accuracy with a fast training time compared to other methods.

6 Conclusion

In this work, we propose DINES, a novel method for learning node representations in signed directed graphs without social assumptions. Our learning framework utilizes a disentangled architecture, specifically designed to learn diverse latent factors of each node through disentangled signed graph convolution layers. To capture the signed relationship between two nodes more effectively, we introduce a novel decoder that leverages pairwise correlations among their disentangled factors, and analyze how our decoding strategy is more effective than the traditional one. We further adopt a self-supervised factor-wise classification to boost the disentanglement of factors. Throughout extensive experiments, we demonstrate that DINES outperforms other state-of-the-art methods in the link sign prediction task, showing linear scalability and a good trade-off between accuracy and time.

References

- [1] Ramanathan V. Guha, Ravi Kumar, Prabhakar Raghavan, and Andrew Tomkins. Propagation of trust and distrust. In *Proceedings of the 13th international conference on World Wide Web, WWW 2004, New York, NY, USA, May 17-20, 2004*, pages 403–412. ACM, 2004. doi: 10.1145/988672.988727. URL <https://doi.org/10.1145/988672.988727>. 1, 12, 24
- [2] Srijan Kumar, Francesca Spezzano, V. S. Subrahmanian, and Christos Faloutsos. Edge weight prediction in weighted signed networks. In *IEEE 16th International Conference on Data Mining, ICDM 2016, December 12-15, 2016, Barcelona, Spain*, pages 221–230. IEEE Computer Society, 2016. doi: 10.1109/ICDM.2016.0033. URL <https://doi.org/10.1109/ICDM.2016.0033>. 1, 11, 23
- [3] Jérôme Kunegis, Andreas Lommatzsch, and Christian Bauckhage. The slashdot zoo: mining a social network with negative edges. In *Proceedings of the 18th International Conference on World Wide Web, WWW 2009, Madrid, Spain, April 20-24, 2009*, pages 741–750. ACM, 2009. doi: 10.1145/1526709.1526809. URL <https://doi.org/10.1145/1526709.1526809>. 1, 11, 23
- [4] Changwon Seo, Kyeong-Joong Jeong, Sungsu Lim, and Won-Yong Shin. Siren: Sign-aware recommendation using graph neural networks. *CoRR*, abs/2108.08735, 2021. URL <https://arxiv.org/abs/2108.08735>. 1
- [5] Jure Leskovec, Daniel P. Huttenlocher, and Jon M. Kleinberg. Signed networks in social media. In *Proceedings of the 28th International Conference on Human Factors in Computing Systems, CHI 2010, Atlanta, Georgia, USA, April 10-15, 2010*, pages 1361–1370. ACM, 2010. doi: 10.1145/1753326.1753532. URL <https://doi.org/10.1145/1753326.1753532>. 1, 2
- [6] Jure Leskovec, Daniel P. Huttenlocher, and Jon M. Kleinberg. Predicting positive and negative links in online social networks. In *Proceedings of the 19th International Conference on World Wide Web, WWW 2010, Raleigh, North Carolina, USA, April 26-30, 2010*, pages 641–650. ACM, 2010. doi: 10.1145/1772690.1772756. URL <https://doi.org/10.1145/1772690.1772756>. 1

-
- [7] Robert West, Hristo S. Paskov, Jure Leskovec, and Christopher Potts. Exploiting social network structure for person-to-person sentiment analysis. *Transactions of the Association for Computational Linguistics*, 2:297–310, 2014. doi: 10.1162/tac1_a_00184. URL https://doi.org/10.1162/tac1_a_00184. 1, 11, 23
 - [8] Jiliang Tang, Yi Chang, Charu C. Aggarwal, and Huan Liu. A survey of signed network mining in social media. *ACM Computing Surveys*, 49(3):42:1–42:37, 2016. doi: 10.1145/2956185. URL <https://doi.org/10.1145/2956185>. 1
 - [9] Dongjin Song, David A. Meyer, and Dacheng Tao. Efficient latent link recommendation in signed networks. In *Proceedings of the 21th ACM SIGKDD International Conference on Knowledge Discovery and Data Mining, Sydney, NSW, Australia, August 10-13, 2015*, pages 1105–1114. ACM, 2015. doi: 10.1145/2783258.2783358. URL <https://doi.org/10.1145/2783258.2783358>. 1
 - [10] Pinghua Xu, Wenbin Hu, Jia Wu, and Bo Du. Link prediction with signed latent factors in signed social networks. In *Proceedings of the 25th ACM SIGKDD International Conference on Knowledge Discovery & Data Mining, KDD 2019, Anchorage, AK, USA, August 4-8, 2019*, pages 1046–1054. ACM, 2019. doi: 10.1145/3292500.3330850. URL <https://doi.org/10.1145/3292500.3330850>. 1, 3, 4, 12, 25
 - [11] Jinhong Jung, Woojeong Jin, and U Kang. Random walk-based ranking in signed social networks: model and algorithms. *Knowledge and Information Systems*, 62(2):571–610, 2020. doi: 10.1007/s10115-019-01364-z. URL <https://doi.org/10.1007/s10115-019-01364-z>. 1
 - [12] Xiaoming Li, Hui Fang, and Jie Zhang. Supervised user ranking in signed social networks. In *The Thirty-Third AAAI Conference on Artificial Intelligence, AAAI 2019, The Thirty-First Innovative Applications of Artificial Intelligence Conference, IAAI 2019, The Ninth AAAI Symposium on Educational Advances in Artificial Intelligence, EAAI 2019, Honolulu, Hawaii, USA, January 27 - February 1, 2019*, pages 184–191. AAAI Press, 2019. doi: 10.1609/aaai.v33i01.3301184. URL <https://doi.org/10.1609/aaai.v33i01.3301184>.
 - [13] Jinhong Jung, Woojeong Jin, Lee Sael, and U Kang. Personalized ranking in signed networks using signed random walk with restart. In *IEEE 16th International Conference on Data Mining, ICDM 2016, December 12-15, 2016, Barcelona, Spain*, pages 973–978. IEEE Computer Society, 2016. doi: 10.1109/ICDM.2016.0122. URL <https://doi.org/10.1109/ICDM.2016.0122>. 1, 4
 - [14] Jiliang Tang, Charu C. Aggarwal, and Huan Liu. Node classification in signed social networks. In *Proceedings of the 2016 SIAM International Conference on Data Mining, Miami, Florida, USA, May 5-7, 2016*, pages 54–62. SIAM, 2016. doi: 10.1137/1.9781611974348.7. URL <https://doi.org/10.1137/1.9781611974348.7>. 1
 - [15] Yixuan He, Gesine Reinert, Songchao Wang, and Mihai Cucuringu. SSSNET: semi-supervised signed network clustering. In *Proceedings of the 2022 SIAM International Conference on Data Mining, SDM 2022, Alexandria, VA, USA, April 28-30, 2022*, pages 244–252. SIAM, 2022. doi: 10.1137/1.9781611977172.28. URL <https://doi.org/10.1137/1.9781611977172.28>. 1
 - [16] Srijan Kumar, Francesca Spezzano, and V. S. Subrahmanian. Accurately detecting trolls in slashdot zoo via decluttering. In *2014 IEEE/ACM International Conference on Advances in Social Networks Analysis and Mining, ASONAM 2014, Beijing, China, August 17-20, 2014*, pages 188–195. IEEE Computer Society, 2014. doi: 10.1109/ASONAM.2014.6921581. URL <https://doi.org/10.1109/ASONAM.2014.6921581>. 1
 - [17] Bo Yang, William K. Cheung, and Jiming Liu. Community mining from signed social networks. *IEEE transactions on knowledge and data engineering*, 19(10):1333–1348, 2007. doi: 10.1109/TKDE.2007.1061. URL <https://doi.org/10.1109/TKDE.2007.1061>. 1
 - [18] Lingyang Chu, Zhefeng Wang, Jian Pei, Jiannan Wang, Zijin Zhao, and Enhong Chen. Finding gangs in war from signed networks. In *Proceedings of the 22nd ACM SIGKDD International Conference on Knowledge Discovery and Data Mining, San Francisco, CA, USA, August 13-17, 2016*, pages 1505–1514. ACM, 2016. doi: 10.1145/2939672.2939855. URL <https://doi.org/10.1145/2939672.2939855>.
 - [19] Ruo-Chun Tzeng, Bruno Ordozgoiti, and Aristides Gionis. Discovering conflicting groups in signed networks. In *Advances in Neural Information Processing Systems 33: Annual*

-
- Conference on Neural Information Processing Systems 2020, NeurIPS 2020, December 6-12, 2020, virtual, 2020.* URL <https://proceedings.neurips.cc/paper/2020/hash/7cc538b1337957dae283c30ad46def38-Abstract.html>. 1
- [20] Yiqi Chen, Tiejun Qian, Huan Liu, and Ke Sun. "bridge": Enhanced signed directed network embedding. In *Proceedings of the 27th ACM International Conference on Information and Knowledge Management, CIKM 2018, Torino, Italy, October 22-26, 2018*, pages 773–782. ACM, 2018. doi: 10.1145/3269206.3271738. URL <https://doi.org/10.1145/3269206.3271738>. 1, 2, 4, 12, 23, 25
 - [21] Shuhan Yuan, Xintao Wu, and Yang Xiang. SNE: signed network embedding. In *Advances in Knowledge Discovery and Data Mining - 21st Pacific-Asia Conference, PAKDD 2017, Jeju, South Korea, May 23-26, 2017, Proceedings, Part II*, volume 10235 of *Lecture Notes in Computer Science*, pages 183–195, 2017. doi: 10.1007/978-3-319-57529-2_15. URL https://doi.org/10.1007/978-3-319-57529-2_15. 3, 4, 12, 25
 - [22] Junghwan Kim, Haekyu Park, Ji-Eun Lee, and U Kang. SIDE: representation learning in signed directed networks. In *Proceedings of the 2018 World Wide Web Conference on World Wide Web, WWW 2018, Lyon, France, April 23-27, 2018*, pages 509–518. ACM, 2018. doi: 10.1145/3178876.3186117. URL <https://doi.org/10.1145/3178876.3186117>. 2, 4, 12, 25
 - [23] Yeon-Chang Lee, Nayoun Seo, Kyungsik Han, and Sang-Wook Kim. Asine: Adversarial signed network embedding. In *Proceedings of the 43rd International ACM SIGIR conference on research and development in Information Retrieval, SIGIR 2020, Virtual Event, China, July 25-30, 2020*, pages 609–618. ACM, 2020. doi: 10.1145/3397271.3401079. URL <https://doi.org/10.1145/3397271.3401079>. 2, 4, 12, 25
 - [24] Pinghua Xu, Yibing Zhan, Liu Liu, Baosheng Yu, Bo Du, Jia Wu, and Wenbin Hu. Dual-branch density ratio estimation for signed network embedding. In *WWW '22: The ACM Web Conference 2022, Virtual Event, Lyon, France, April 25 - 29, 2022*, pages 1651–1662. ACM, 2022. doi: 10.1145/3485447.3512171. URL <https://doi.org/10.1145/3485447.3512171>. 1, 2, 4, 12, 25
 - [25] Tyler Derr, Yao Ma, and Jiliang Tang. Signed graph convolutional networks. In *IEEE International Conference on Data Mining, ICDM 2018, Singapore, November 17-20, 2018*, pages 929–934. IEEE Computer Society, 2018. doi: 10.1109/ICDM.2018.00113. URL <https://doi.org/10.1109/ICDM.2018.00113>. 1, 2, 4, 6, 8, 10, 12, 25
 - [26] Yu Li, Yuan Tian, Jiawei Zhang, and Yi Chang. Learning signed network embedding via graph attention. In *The Thirty-Fourth AAAI Conference on Artificial Intelligence, AAAI 2020, The Thirty-Second Innovative Applications of Artificial Intelligence Conference, IAAI 2020, The Tenth AAAI Symposium on Educational Advances in Artificial Intelligence, EAAI 2020, New York, NY, USA, February 7-12, 2020*, pages 4772–4779. AAAI Press, 2020. URL <https://ojs.aaai.org/index.php/AAAI/article/view/5911>. 2, 4, 6, 8, 12, 24, 25
 - [27] Haoxin Liu, Ziwei Zhang, Peng Cui, Yafeng Zhang, Qiang Cui, Jiashuo Liu, and Wenwu Zhu. Signed graph neural network with latent groups. In *KDD '21: The 27th ACM SIGKDD Conference on Knowledge Discovery and Data Mining, Virtual Event, Singapore, August 14-18, 2021*, pages 1066–1075. ACM, 2021. doi: 10.1145/3447548.3467355. URL <https://doi.org/10.1145/3447548.3467355>. 3, 4, 12, 24, 25
 - [28] Lin Shu, Erxin Du, Yaomin Chang, Chuan Chen, Zibin Zheng, Xingxing Xing, and Shaofeng Shen. SGCL: contrastive representation learning for signed graphs. In *CIKM '21: The 30th ACM International Conference on Information and Knowledge Management, Virtual Event, Queensland, Australia, November 1 - 5, 2021*, pages 1671–1680. ACM, 2021. doi: 10.1145/3459637.3482478. URL <https://doi.org/10.1145/3459637.3482478>. 4, 6, 8, 10, 12, 25
 - [29] Junjie Huang, Huawei Shen, Liang Hou, and Xueqi Cheng. SDGNN: learning node representation for signed directed networks. In *Thirty-Fifth AAAI Conference on Artificial Intelligence, AAAI 2021, Thirty-Third Conference on Innovative Applications of Artificial Intelligence, IAAI 2021, The Eleventh Symposium on Educational Advances in Artificial Intelligence, EAAI 2021, Virtual Event, February 2-9, 2021*, pages 196–203. AAAI Press, 2021. URL <https://ojs.aaai.org/index.php/AAAI/article/view/16093>. 2, 4, 5, 12, 23, 25

-
- [30] Jinhong Jung, Jaemin Yoo, and U. Kang. Signed random walk diffusion for effective representation learning in signed graphs. *PLOS ONE*, 17(3):1–19, 03 2022. doi: 10.1371/journal.pone.0265001. URL <https://doi.org/10.1371/journal.pone.0265001>. 2, 4, 6, 8, 10, 12, 23, 24, 25
 - [31] Dengcheng Yan, Youwen Zhang, Wenxin Xie, Ying Jin, and Yiwen Zhang. MUSE: multi-faceted attention for signed network embedding. *Neurocomputing*, 519:36–43, 2023. doi: 10.1016/j.neucom.2022.11.021. URL <https://doi.org/10.1016/j.neucom.2022.11.021>. 2, 3, 4, 10, 12, 24, 25
 - [32] Stefano Fiorini, Stefano Coniglio, Michele Ciavotta, and Enza Messina. Sigmanet: One laplacian to rule them all. *CoRR*, abs/2205.13459, 2022. doi: 10.48550/arXiv.2205.13459. URL <https://doi.org/10.48550/arXiv.2205.13459>. 1, 3, 4, 12, 25
 - [33] Dorwin Cartwright and Frank Harary. Structural balance: a generalization of heider’s theory. *Psychological review*, 63(5):277, 1956. 2
 - [34] Géraud Le Falher. *Characterizing Edges in Signed and Vector-Valued Graphs. (Caractérisation des arêtes dans les graphes signés et attribués)*. PhD thesis, Lille University of Science and Technology, France, 2018. URL <https://tel.archives-ouvertes.fr/tel-01824215>. 2
 - [35] James A Davis. Clustering and structural balance in graphs. *Human relations*, 20(2):181–187, 1967. 2
 - [36] Jianxin Ma, Peng Cui, Kun Kuang, Xin Wang, and Wenwu Zhu. Disentangled graph convolutional networks. In *Proceedings of the 36th International Conference on Machine Learning, ICML 2019, 9-15 June 2019, Long Beach, California, USA*, volume 97 of *Proceedings of Machine Learning Research*, pages 4212–4221. PMLR, 2019. URL <http://proceedings.mlr.press/v97/ma19a.html>. 3, 4, 5, 6, 10, 12, 25
 - [37] Yanbei Liu, Xiao Wang, Shu Wu, and Zhitao Xiao. Independence promoted graph disentangled networks. In *The Thirty-Fourth AAAI Conference on Artificial Intelligence, AAAI 2020, The Thirty-Second Innovative Applications of Artificial Intelligence Conference, IAAI 2020, The Tenth AAAI Symposium on Educational Advances in Artificial Intelligence, EAAI 2020, New York, NY, USA, February 7-12, 2020*, pages 4916–4923. AAAI Press, 2020. URL <https://ojs.aaai.org/index.php/AAAI/article/view/5929>. 3, 4, 6, 10
 - [38] Thomas N. Kipf and Max Welling. Semi-supervised classification with graph convolutional networks. In *5th International Conference on Learning Representations, ICLR 2017, Toulon, France, April 24-26, 2017, Conference Track Proceedings*. OpenReview.net, 2017. URL <https://openreview.net/forum?id=SJU4ayYgl>. 4, 8
 - [39] Johannes Klicpera, Aleksandar Bojchevski, and Stephan Günnemann. Predict then propagate: Graph neural networks meet personalized pagerank. In *7th International Conference on Learning Representations, ICLR 2019, New Orleans, LA, USA, May 6-9, 2019*. OpenReview.net, 2019. URL <https://openreview.net/forum?id=H1gL-2A9Ym>. 4
 - [40] Suhang Wang, Jiliang Tang, Charu C. Aggarwal, Yi Chang, and Huan Liu. Signed network embedding in social media. In *Proceedings of the 2017 SIAM International Conference on Data Mining, Houston, Texas, USA, April 27-29, 2017*, pages 327–335. SIAM, 2017. doi: 10.1137/1.9781611974973.37. URL <https://doi.org/10.1137/1.9781611974973.37>. 4
 - [41] Xiang Wang, Hongye Jin, An Zhang, Xiangnan He, Tong Xu, and Tat-Seng Chua. Disentangled graph collaborative filtering. In *Proceedings of the 43rd International ACM SIGIR conference on research and development in Information Retrieval, SIGIR 2020, Virtual Event, China, July 25-30, 2020*, pages 1001–1010. ACM, 2020. doi: 10.1145/3397271.3401137. URL <https://doi.org/10.1145/3397271.3401137>. 4
 - [42] Tianxiang Zhao, Xiang Zhang, and Suhang Wang. Exploring edge disentanglement for node classification. In *WWW ’22: The ACM Web Conference 2022, Virtual Event, Lyon, France, April 25 - 29, 2022*, pages 1028–1036. ACM, 2022. doi: 10.1145/3485447.3511929. URL <https://doi.org/10.1145/3485447.3511929>. 4, 10
 - [43] William L. Hamilton, Zhitao Ying, and Jure Leskovec. Inductive representation learning on large graphs. In *Advances in Neural Information Processing Systems 30: Annual Conference on Neural Information Processing Systems 2017, December 4-9, 2017, Long Beach, CA, USA*,

-
- pages 1024–1034, 2017. URL <https://proceedings.neurips.cc/paper/2017/hash/5dd9db5e033da9c6fb5ba83c7a7e9bea9-Abstract.html>. 7, 9
- [44] Keyulu Xu, Weihua Hu, Jure Leskovec, and Stefanie Jegelka. How powerful are graph neural networks? In *7th International Conference on Learning Representations, ICLR 2019, New Orleans, LA, USA, May 6-9, 2019*. OpenReview.net, 2019. URL <https://openreview.net/forum?id=ryGs6iA5Km>. 8, 9, 15
 - [45] Bryan Perozzi, Rami Al-Rfou, and Steven Skiena. Deepwalk: online learning of social representations. In *The 20th ACM SIGKDD International Conference on Knowledge Discovery and Data Mining, KDD '14, New York, NY, USA - August 24 - 27, 2014*, pages 701–710. ACM, 2014. doi: 10.1145/2623330.2623732. URL <https://doi.org/10.1145/2623330.2623732>. 12
 - [46] Jian Tang, Meng Qu, Mingzhe Wang, Ming Zhang, Jun Yan, and Qiaozhu Mei. LINE: large-scale information network embedding. In *Proceedings of the 24th International Conference on World Wide Web, WWW 2015, Florence, Italy, May 18-22, 2015*, pages 1067–1077. ACM, 2015. doi: 10.1145/2736277.2741093. URL <https://doi.org/10.1145/2736277.2741093>. 12
 - [47] Aditya Grover and Jure Leskovec. node2vec: Scalable feature learning for networks. In *Proceedings of the 22nd ACM SIGKDD International Conference on Knowledge Discovery and Data Mining, San Francisco, CA, USA, August 13-17, 2016*, pages 855–864. ACM, 2016. doi: 10.1145/2939672.2939754. URL <https://doi.org/10.1145/2939672.2939754>. 12
 - [48] Andrew P. Bradley. The use of the area under the ROC curve in the evaluation of machine learning algorithms. *Pattern Recognition*, 30(7):1145–1159, 1997. doi: 10.1016/S0031-3203(96)00142-2. URL [https://doi.org/10.1016/S0031-3203\(96\)00142-2](https://doi.org/10.1016/S0031-3203(96)00142-2). 12
 - [49] Abdel Aziz Taha and Allan Hanbury. Metrics for evaluating 3D medical image segmentation: analysis, selection, and tool. *BMC medical imaging*, 15:29, 2015. 12
 - [50] Jure Leskovec, Daniel P. Huttenlocher, and Jon M. Kleinberg. Predicting positive and negative links in online social networks. In *Proceedings of the 19th International Conference on World Wide Web, WWW 2010, Raleigh, North Carolina, USA, April 26-30, 2010*, pages 641–650. ACM, 2010. doi: 10.1145/1772690.1772756. URL <https://doi.org/10.1145/1772690.1772756>. 15
 - [51] Laurens Van der Maaten and Geoffrey Hinton. Visualizing data using t-SNE. *Journal of machine learning research*, 9(11), 2008. 16
 - [52] Peter J Rousseeuw. Silhouettes: A graphical aid to the interpretation and validation of cluster analysis. *Journal of computational and applied mathematics*, 20:53–65, 1987. 17
 - [53] Jinhong Jung, Ha-Myung Park, and U Kang. Balansing: Fast and scalable generation of realistic signed networks. In *Proceedings of the 23rd International Conference on Extending Database Technology, EDBT 2020, Copenhagen, Denmark, March 30 - April 02, 2020*, pages 193–204. OpenProceedings.org, 2020. doi: 10.5441/002/edbt.2020.18. URL <https://doi.org/10.5441/002/edbt.2020.18>. 17

A Appendix

A.1 Time Complexity Analysis

Table 7: Time complexity of each component of DINES where L , d , and K are hyperparameters (see Table 1), and they are set to constants much smaller than the numbers n and m of nodes and edges, respectively.

Components	References	Time Complexities
Encoder	Algorithm 1	$O(L \frac{d^2}{K} m + L \frac{d^2}{K} n)$
Decoder	Algorithm 2	$O(dKm)$
\mathcal{L}_{bce}	Equation (8)	$O(m)$
\mathcal{L}_{disc}	Equation (10)	$O(dKn)$
Total Complexity		$O(L \frac{d^2}{K} m + L \frac{d^2}{K} n + dKn)$
Simplified Complexity		$O(m + n)$

Lemma 1 (Time Complexity of Encoder of DINES). *The time complexity of Algorithm 1 takes $O(L \frac{d^2}{K} m + L \frac{d^2}{K} n)$ time.*

Proof. For each node u , the initial disentanglement (lines 1-5) takes $O(d^2 |\mathcal{N}_u|)$ time (i.e., $O(d^2 m)$ time is required for all nodes). For each factor k , the *dsg-conv* layer consists of three operations called *aggregate_k*, *update_k*, and *normalize_k*. For the *aggregate_k*(\cdot) (line 14), the sum, mean, and max functions take $O(|\mathcal{N}_u| \frac{d}{K})$ time while the attention function requires $O(|\mathcal{N}_u| \frac{d^2}{K^2})$ time where $|\mathcal{N}_u^\delta| \leq |\mathcal{N}_u|$. Considering the aforementioned aggregators, the time complexity of *aggregate_k*(\cdot) is up to $O(|\mathcal{N}_u| \frac{d^2}{K^2})$. The *update_k*(\cdot) and *normalize_k*(\cdot) take $O(\frac{d^2}{K^2})$ and $O(\frac{d}{K})$ time due to the fully-connected layer and the l_2 -normalization, respectively. Overall, the encoder takes $O(L \frac{d^2}{K} |\mathcal{N}_u| + L \frac{d^2}{K})$ time for each node as it repeats the *dsg-conv* layer LK times. For all nodes, it exhibits $O(L \frac{d^2}{K} m + L \frac{d^2}{K} n)$ time cost because $\sum_{u \in \mathcal{V}} |\mathcal{N}_u| = O(m)$.

Lemma 2 (Time Complexity of Decoder of DINES). *The time complexity of Algorithm 2 takes $O(dKm)$ time.*

Proof. For each edge $u \rightarrow v$, it takes $O(d)$ time to build \mathbf{Z}_u and \mathbf{Z}_v (line 2). Computing the correlations takes $O(dK)$ time where each inner product takes $O(\frac{d}{K})$ time (line 3). It consumes $O(K^2)$ time to compute the probability p_{uv} (line 4). For all given edges (lines 1-5), our decoder takes $O(dKm + K^2m) = O(dKm)$ time where $K \leq d$.

A.2 Details of Datasets

We describe more details of the datasets used in the paper as follows:

- **BC-Alpha**⁵ and **BC-OTC**⁶ [2]: These are who-trusts-whom networks of users on Bitcoin platforms where transactions occur anonymously. They allow users to give other users a score between -10 (distrust) and 10 (trust) to reveal fraudulent users. As in [29, 30], we also regard links whose scores are higher than zero as positive edges; otherwise, they are considered negative edges.
- **Wiki-RFA**⁷ [7]: This is a signed network in Wikipedia where users vote for administrator candidates. The users can cast for or against candidates. The site allowed users to express neutral opinions about the candidates, but few users gave neutral votes. As in [20, 29], we also eliminate the neutral votes.
- **Slashdot**⁸ [3]: This is a signed social network on Slashdot, a technology news website. The site introduced a tagging system that allows users to tag other users as friends or foes; thus, the signed graph is represented as trust relationships between the users.

⁵<https://snap.stanford.edu/data/soc-sign-bitcoin-alpha.html>

⁶<https://snap.stanford.edu/data/soc-sign-bitcoin-otc.html>

⁷<https://snap.stanford.edu/data/wiki-RfA.html>

⁸<http://konect.cc/networks/slashdot-zoo>

- **Epinions**⁹ [1]: This is an online social network on Epinions, a general consumer review site. On the website, users can decide whether to trust each other, and the signed graph represents such trust relationships.

Note that following previous work on signed GNNs [26, 27, 30], we utilize truncated singular vector decomposition (TSVD) to generate node features because the aforementioned datasets do not contain initial node features. Specifically, suppose $\mathbf{X} \in \mathbb{R}^{n \times d}$ denotes a matrix of node features. Then, we set $\mathbf{X} = \mathbf{U}\Sigma_d$ where a signed adjacency matrix \mathbf{A} is decomposed by TSVD as $\mathbf{A} \simeq \mathbf{U}\Sigma_d\mathbf{V}^\top$. We follow their setup and extract the initial node features with target rank $d = 64$ for each dataset.

A.3 Hyperparameters of DINES

We report the results of the cross-validation that searches for the hyperparameters of DINES (see the symbols in Table 1). After repeating the experiments with 10 different random seeds, we select one validated setting that produces a test accuracy closest to the average test accuracy for each metric. The searched hyperparameters are summarized in Tables 8 and 9 for AUC and Macro-F1, respectively.

Table 8: Searched hyperparameters of DINES in terms of AUC.

Dataset	L	K	d_{out}	λ_{disc}	η	λ_{reg}
BC-Alpha	2	8	64	0.1	0.01	0.005
BC-OTC	2	8	64	0.1	0.005	0.01
Wiki-RFA	2	8	64	0.1	0.005	0.005
Slashdot	2	8	64	0.5	0.01	0.01
Epinions	2	8	64	0.1	0.005	0.005

Table 9: Searched hyperparameters of DINES in terms of Macro-F1.

Dataset	L	K	d_{out}	λ_{disc}	η	λ_{reg}
BC-Alpha	2	16	64	0.1	0.005	0.005
BC-OTC	2	8	64	0.1	0.005	0.005
Wiki-RFA	2	16	64	0.1	0.005	0.005
Slashdot	2	8	64	0.1	0.005	0.01
Epinions	2	8	64	0.1	0.005	0.01

A.4 Implementation Information of Competitors

For our experiments, we utilized the open-source implementation provided by the authors for the competing methods, and the URLs for each implementation are as follows:

- **SNE**: <https://bit.ly/42gn9S0>
- **SIDE**: <https://datalab.snu.ac.kr/side/resources/side.zip>
- **BESIDE**: <https://github.com/yqc01/BESIDE>
- **SLF**: <https://github.com/WHU-SNA/SLF>
- **ASiNE**: <https://github.com/yeonchang/ASiNE>
- **DDRE**: <https://github.com/XphYYYYYYY/DDRE>
- **SGCN**: <https://github.com/benedekrozemberczki/SGCN>
- **DisenGCN**: <https://github.com/snudatalab/SidNet>
- **SNEA**: <https://github.com/liyu1990/snea>
- **SGCL**: <https://github.com/xi0927/SGCL>
- **GS-GNN**: <https://github.com/haoxin1998/GS-GNN>
- **SDGNN**: <https://bit.ly/45Ifmzj>
- **SIDNET**: <https://github.com/snudatalab/SidNet>
- **MUSE**¹⁰: <https://bit.ly/45TLKPv>
- **SigMaNet**: <https://github.com/Stefa1994/SigMaNet>

⁹<https://snap.stanford.edu/data/soc-sign-epinions.html>

¹⁰The original code for MUSE was not publicly available; thus, we carefully implemented MUSE based on the description in [31], and made our implementation open-source for reproducibility.

A.5 Properties of Learning Models

We compare DINES with other learning models in terms of the following properties:

- (P1) Does a model use the information from edge signs for its learning?
- (P2) Does a model consider the direction of an edge for its learning?
- (P3) Does a model train a signed graph and the link sign prediction task in an end-to-end manner?
- (P4) Is a model free from social theories (e.g., the balance or status theory) for designing its input, model, convolution, or loss?
- (P5) Does a model produce disentangled node representations?

We summarize the comparisons in Table 10. Note that only our method DINES satisfies all of the properties.

Table 10: Properties of learning models related to DINES.

Category	Methods	(P1)	(P2)	(P3)	(P4)	(P5)
Network Embedding	SNE [21]	✓	✓	✗	✓	✗
	SIDE [22]	✓	✓	✗	✗	✗
	BESIDE [20]	✓	✓	✗	✗	✗
	SLF [10]	✓	✓	✗	✓	✗
	ASiNE [23]	✓	✗	✗	✗	✗
	DDRE [24]	✓	✓	✗	✗	✗
Graph Neural Networks	SGCN [25]	✓	✗	✓	✗	✗
	DisenGCN [36]	✗	✗	✓	✓	✓
	SNEA [26]	✓	✗	✓	✗	✗
	GS-GNN [27]	✓	✗	✓	✓	✗
	SGCL [28]	✓	✓	✓	✗	✗
	SDGNN [29]	✓	✓	✓	✗	✗
	SIDNET [30]	✓	✓	✓	✗	✗
	MUSE [31]	✓	✗	✓	✗	✓
	SigMaNet [32]	✓	✓	✓	✓	✗
	DINES (ours)	✓	✓	✓	✓	✓

A.6 Further Inspection of Aggregators

We inspect the ability of aggregators such as sum, mean, max, and attention to effectively capture information related to node degrees. For each $\delta \in \mathcal{D}$ and node $u \in \mathcal{V}$, we measure the correlation between the norm of $\|_{k \in K} \mathbf{m}_{u,k}^\delta$ and the degree $|\mathcal{N}_u^\delta|$ where $\mathbf{m}_{u,k}^\delta$ is the message obtained from an aggregator. The results are demonstrated in Figure 10 for all datasets where as the correlation approaches +1, the norm of the concatenated message becomes distinguishable based on the node degree. Note that only the sum aggregator demonstrates a nearly perfect positive correlation. This discrepancy arises because the normalization techniques used by the other aggregators introduce a smoothing effect on the local neighboring structure. In contrast, the sum aggregator avoids this

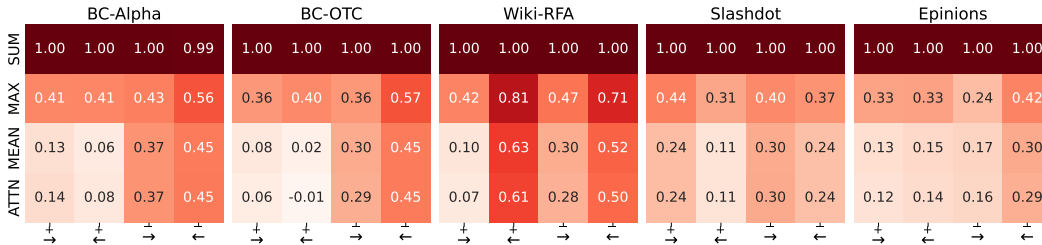


Figure 10: Correlations between the norm of the concatenated message of each aggregator (sum, max, mean, and attention) and the degree of δ -neighbors where $\delta \in \mathcal{D} = \{\rightarrow, \leftarrow, \leftrightarrow, \nleftrightarrow\}$.

smoothing effect, enabling it to capture the local structure more effectively. Thus, the sum aggregator effectively distributes the degree information throughout the messages, resulting in more expressive features compared to the others when learning the signed graphs.

A.7 Effect of Number of Factors

We investigate the effect of the number K of factors in the different dimension d_{out} . When $d_{out} = 64$, the performance of AUC initially improves as the value of K increases while the accuracy starts to decrease after $K = 16$, as shown in Figure 11(a). The reasons for this are twofold: firstly, $\frac{d_{out}}{K}$ is too small to adequately model the features of each factor, and secondly, it becomes challenging to properly capture the information from neighboring nodes within the limited feature size. However, by increasing the dimension d_{out} and enlarging the size of each factor's feature, the performance consistently improves as K increases, as shown in Figures 11(b) and 11(c).

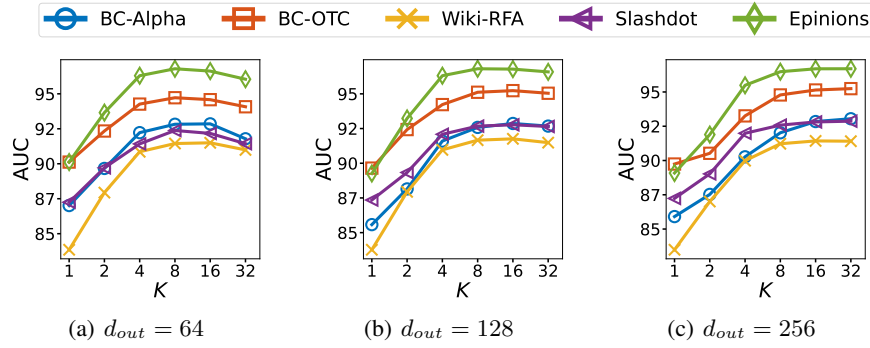


Figure 11: Effects of the number K of factors of DINES in the different dimension d_{out} .